

EVALUATION OF LOW-K DIELECTRIC COMPOSITIONS

EVALUATION OF LOW-K DIELECTRIC COMPOSITIONS
WITH
PLATINUM-SILVER ELECTRODES

By

MICHAEL ERNEST MILLS, B.Sc.

A Thesis

Submitted to the School of Graduate Studies
in Partial Fulfilment of the Requirements
for the Degree
Master of Engineering

McMaster University

September 1977

MASTER OF ENGINEERING (1977)
(Engineering Physics)

McMASTER UNIVERSITY
Hamilton, Ontario

TITLE: Evaluation of Low-K Dielectric Compositions
with Platinum-Silver Electrodes

AUTHOR: Michael Ernest Mills, B.Sc. (Bristol University, U.K.)

SUPERVISOR: Dr. J. Shewchun

NUMBER OF PAGES: x, 70

ABSTRACT

Thick-film dielectric compositions which devitrify in a controlled way to form a ceramic phase during processing, are available for evaluation as crossover insulation in multilayer circuits. Their advantage over compositions based upon a borosilicate glass is that they provide a surface of greater mechanical stability for successive conductor layers during subsequent firing processes. This results in close alignment being maintained between successive layers of a multilayer circuit.

A substantial part of the total manufacturing cost of a thick-film circuit is associated with the noble-metal content of conductor compositions. This has given impetus to the development of Platinum-Silver based pastes in preference to those containing higher percentages of Gold and Palladium. The results of an evaluation of dielectric behaviour using Platinum-Gold electrodes are of little significance if the intention is to use that same dielectric with Platinum-Silver electrodes in production. The interaction of materials at the interfaces during processing is known to alter the properties of the dielectric quite significantly, and the crossover structure must be evaluated as a system if useful data is to be obtained.

This project is an evaluation of two multilayer systems based upon proprietary pastes from two different manufacturers; the dielectric is of the glass-ceramic type and the conductor is based upon a Platinum-Silver composition. Although claims are made in the product literature that both systems have equivalent performance, this report will show substantial differences exist when tests are conducted under the kind of conditions experienced during production.

ACKNOWLEDGEMENT

This Industrial project, which formed part of the requirements for the M. Eng. Degree of the Engineering Physics Department, McMaster University, was undertaken at the Micro-electronic production facilities of Garrett Manufacturing Ltd.

I would like to take this opportunity to express my thanks to the Staff Supervisor for the project at Garrett Manufacturing, Mr. S. Bowen, and to acknowledge the assistance of Mr. J. Malcolm and Mr. D. Goswami.

I am grateful for the helpful suggestions made by Dr. J. Shewchun, my Supervising Professor at McMaster University, Hamilton, Ontario.

TABLE OF CONTENTS

PAGE

Abstract	iii
Acknowledgement	v
List of Illustrations	vii
List of Symbols	x
Introduction	1
Discussion	10
Procedure	23
Results	34
Conclusions	62
Recommendations	66
Appendix	68
References	70

LIST OF ILLUSTRATIONS

FIGURE	TITLE	PAGE
1	Standard firing profile	2
2	Test pattern (x2 magnification)	6
3	DC response of a crossover dielectric	13
4	Equivalent circuit-model for a printed crossover	20
5	Positive film masters	25
6	Processing sequences	27
7	Cross-section through a printed crossover	29
8	Measurement of leakage current	32
9	Location of short-circuits on arrays processed with System 'A' materials	35
10	Location of short-circuits on cross- overs/capacitors for System 'A'	36
11	Location of short-circuits on arrays processed with System 'B' materials	37
12	Location of short-circuits on cross- overs/capacitors for System 'B'	38
13	Effect of re-firing for System 'A', (Option 1(a))	40

FIGURE	TITLE	PAGE
14	Effect of re-firing for System 'A', (Option 2(a))	41
15	Effect of re-firing on arrays processed with System 'B' materials	42
16	Effect of re-firing on crossovers/ capacitors for System 'B'	43
17	Effect of water absorption on insulation resistance (System 'A')	45
18	Insulation resistance (System 'B')	47
19	Effect of water absorption on insulation resistance (System 'B')	48
20(a)	100/600V dielectric strength test results (dry)	49
20(b)	100/600V dielectric strength test results (wet)	49
21	Effects of re-firing once on insulation resistance	52
22	Effects of re-firing once on samples which had previously a short-circuit	54
23	Effect of re-firing three times on insulation resistance	55
24	Unit-area capacitance for System 'A' and System 'B'	56
25	Aging effects over a period of three months	58

FIGURE	TITLE	PAGE
26	Effect of re-firing once on nominal capacitance values	58
27	Variation of dielectric constant with frequency	59
28	Variation in ac loss with frequency	61
29	The Q-meter circuit	69

TABLE	TITLE	PAGE
1	Test pattern dimensions	7
2	Substrate code-numbers for processing options	30

LIST OF SYMBOLS

A, B..N	identification labels on test pattern
$A_1, A_2 \dots A_{30}$	substrate coding for System 'A'
$B_1, B_2 \dots B_{20}$	substrate coding for System 'B'
B_c	susceptance of equivalent parallel capacitor
C	equivalent parallel capacitor
C_1, C_2	tuning-capacitor settings for Q-meter measurement
C_x	coupling capacitance of a single crossover
G	conductance of equivalent parallel resistor
i_a	absorption current
i_l	leakage current
j	complex operator
K	dielectric constant
L	inductance (model parameter)
Q_1, Q_2	Q-meter readings
Q	$Q_1 - Q_2$
R	equivalent parallel resistor
R_p	shunt resistive loss (model parameter)
R_s	series resistive loss (model parameter)
δ	loss angle
ω	angular frequency

INTRODUCTION

Thick-film technology is based upon a screen-printing process in which conductor, resistor and dielectric compositions in paste form can be selectively printed through selected areas of a masked stainless-steel mesh screen on to an alumina substrate. Freshly printed substrates are placed in a dust-free cabinet to allow the screen impression marks to disappear, and the pattern surfaces to become smooth and glossy. These printed substrates are then dried in an oven, typically for 15 minutes at a temperature of 150°C , which removes the volatile solvent which made the paste screenable. The next step involves a higher temperature firing operation, which in the case of the compositions used in this evaluation requires a peak temperature of 850°C . As the substrates pass through the furnace on a conveyor belt, their temperature follows the firing profile illustrated in Figure 1. As the temperature rises, the organic binder burns off and is carried away by convection currents through the furnace tube. During the temperature plateau at 850°C the glass frit component melts so that the solid components can diffuse and blend together, and special nucleating agents encourage the formation of a polycrystalline ceramic phase. During the cooling-down period, this ceramic phase becomes securely bonded to the substrate by means of the glass matrix.

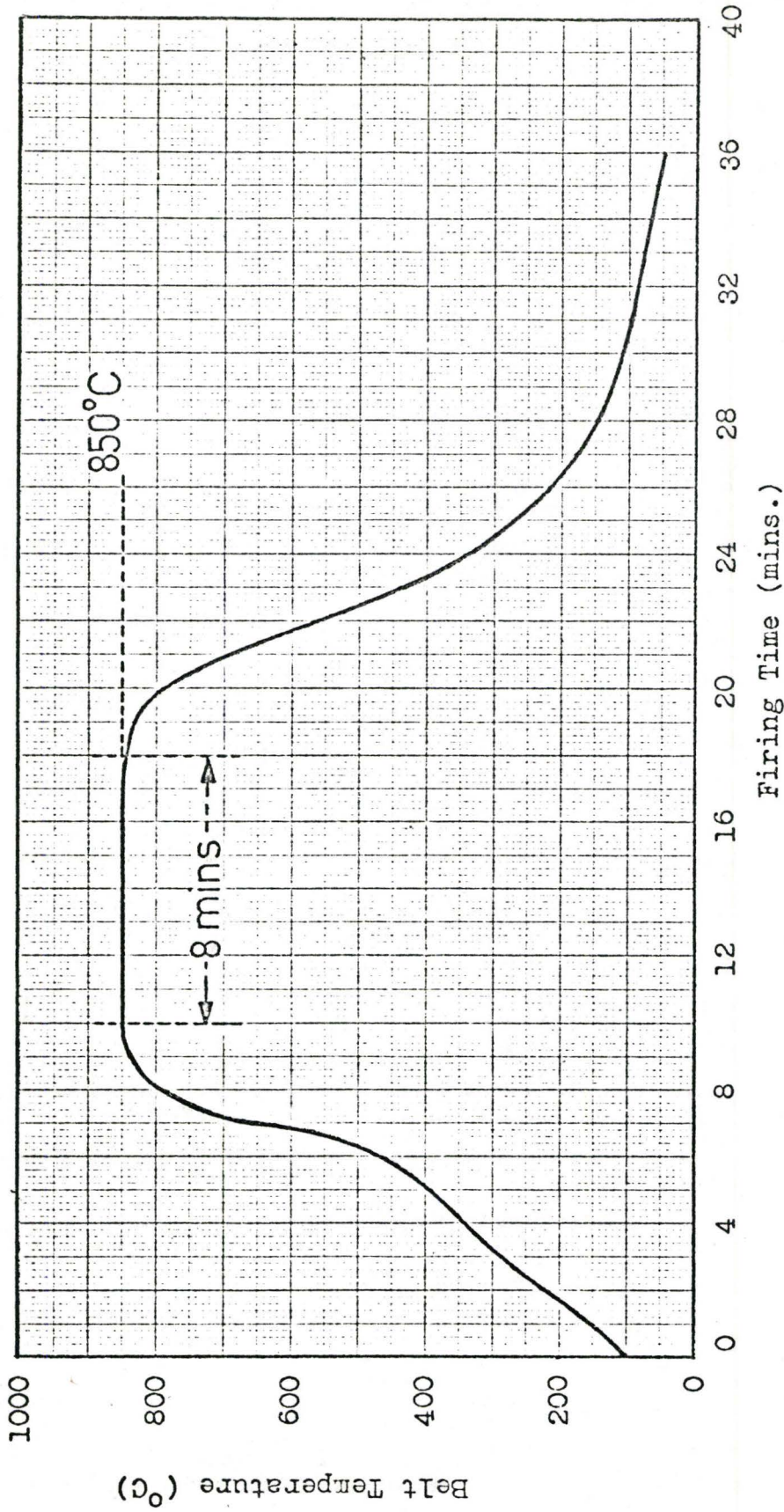


Figure 1. Standard firing profile.

The choice of paste, and the sequence in which each one is printed and fired, depends upon the components needed in the multilayer circuit. If the composition of the paste contains finely dispersed Silver, Platinum, Palladium or Gold, the fired pattern can be made conductive. If the composition includes such oxides as, for example, Palladium Oxide or Ruthenium Oxide, the conductivity can be reduced by many orders of magnitude and the fired pattern becomes resistive. It follows that a useful dielectric can be formed by omitting the metals and these oxides, retaining the glass-ceramic components. An arrangement in which one conductor of a circuit must be insulated from another passing over it occurs often in the design of a multilayer circuit, and is referred to as a "crossover". The lower conductor is printed and fired first. This is generally followed by a double-print of dielectric which is then co-fired with the upper conductor which has been printed over the dielectric. If resistors of low value are required, they are printed and fired next, followed by those of high value. This sequence tends to reduce the drift in value which is experienced by subsequent firing and which is more severe for the higher value resistors. Capacitors of low value can obviously be designed in parallel-plate format using the low dielectric constant insulation of the crossover as the capacitor dielectric, in which case they can be printed and fired along with the crossovers. For larger values, a high dielectric constant composition can be

substituted at the appropriate printing stage.

A set of conductor, resistor and dielectric pastes from a given manufacturer is referred to as "compatible" if the glass components in each of the pastes will combine on firing to produce an interface which is free of occluded gas. The overall performance of a compatible paste system depends very much on the equipment and technique used to prepare test samples, and consequently the choice of a suitable system cannot be made on the basis of information in the product literature alone. The exact composition of each paste is not usually divulged by the manufacturer for proprietary reasons, making it rather difficult to interpret the results of an "in-house" evaluation except in somewhat general terms. Fortunately, as far as a microcircuit manufacturer is concerned, the most meaningful data is obtained by utilising a test pattern which in all respects typifies the problems expected in circuit production. Compatible paste systems can then be evaluated on the same terms, revealing features of the materials which may not be apparent in some of the more "idealised" laboratory tests. This explains why so much reliance is placed upon the kind of test procedure illustrated in this report for two compatible systems from different suppliers, and for which the data in the product literature appears to be very similar in all respects. This report demonstrates considerable differences between such systems when evaluated for production work in thick-film technology.

For the two systems evaluated in this report, certain constraints were established. Since it is well known in thick-film technology that the electrical properties of a dielectric layer are sensitive to printing and firing conditions in particular, the same printing screens and firing profile were used for all test substrates. From the production standpoint, it is advantageous for successive printings of conductor and dielectric in a multilayer circuit to be fired at the same temperature profile. This avoids the delay incurred when furnaces have to be reset and left to stabilise. Furthermore, this takes advantage of one of the properties of the new glass-ceramic compositions, namely that the melting point after being fired once is somewhat higher than before because of the ceramic phase developed; refiring at the same profile several times thereafter does not reflow the dielectric layer, and the registration of the conductor layers is maintained to closer tolerance than that achieved with a borosilicate glass.

All of the test substrates for both paste systems were prepared using the test pattern illustrated in Figure 2, and dimensioned in Table 1. The pattern includes a variety of different sized parallel-plate format capacitors (labelled "A" through "J"), several crossovers (labelled "K" through "N") and a large area consisting of identically sized and closely spaced crossovers in the form of an "array". Some of the substrates utilised the entire pattern because they were

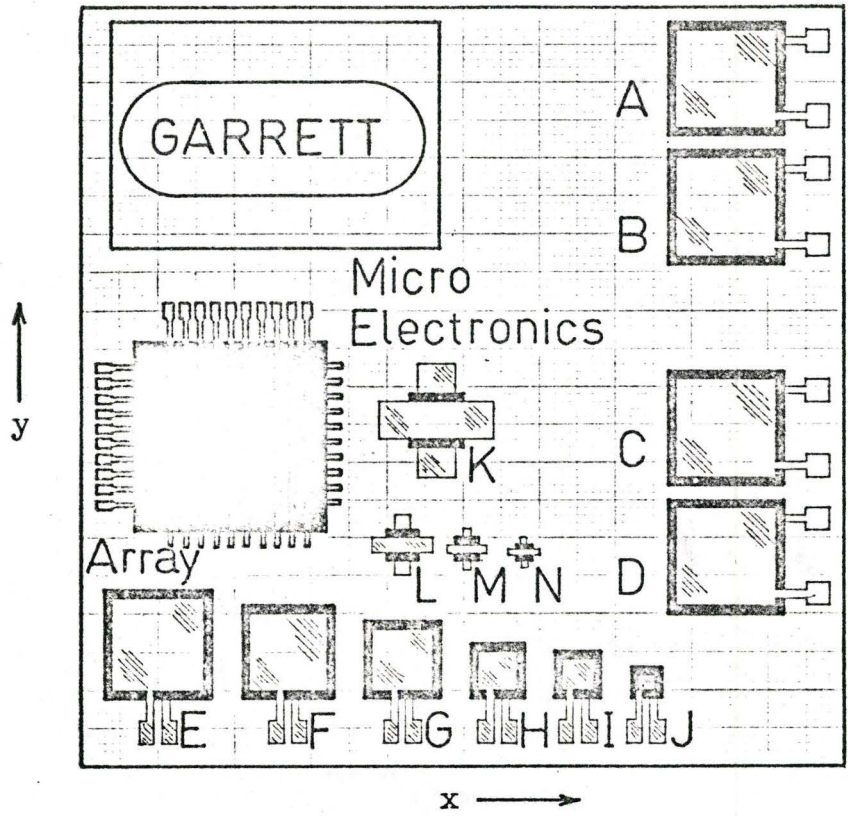


Figure 2. Test pattern. (x2 magnification)

- Conductor
- Dielectric

Location of Pad	Electrodes		Dielectric	
	x (mm)	y (mm)	x (mm)	y (mm)
A,B,C,D,E	6.37	6.37	7.36	7.36
F	5.10	5.10	6.08	6.08
G	3.82	3.82	4.82	4.82
H	2.53	2.53	3.54	3.54
I	1.79	1.79	2.75	2.75
J	1.26	1.26	2.23	2.23
K	2.54	7.66	3.57	3.57
L	1.24	3.82	2.27	2.27
M	0.61	2.55	1.62	1.62
N	0.24	2.16	1.22	1.22
Array	0.27	0.27 *	—	—

* Dimensions of a single crossover

Table 1. Test pattern dimensions.

2" x 2", whereas the 1" x 1" substrates utilised only the array, with the remainder of the pattern being blanked off. At the request of Garrett Manufacturing, the identity of the paste systems was not to be disclosed for proprietary reasons, and so the two systems selected had to be described as System 'A' and System 'B', each consisting of one conductor and one dielectric paste.

Comparative measurements were made on the thick-film test substrates prepared from the materials of both systems, under the following headings. In some cases, the interpretation of the measurements in the thick-film Industry is based upon an 'operational definition' which may differ from the accepted meaning in the Electrical Engineering field:

Dielectric Integrity

- identification of the number and location of any short-circuited crossovers on the array of each test substrate, to predict the likely yield of acceptable circuits in production.
- investigation of the effects of multiple refiring on the overall yield.

Insulation Resistance

- measurement of the conductivity of the crossover dielectric under dc conditions.
- the effect of water absorption on the insulation resistance at different dc voltage levels.
- the effect of refiring on dielectrics previously

exposed to water.

Dielectric Strength

- non-destructive testing in which the insulation resistance is measured at 100V dc and then compared to its value at 600V dc; the increase in conductivity (assuming no breakdown) should not exceed three orders-of-magnitude for its dielectric strength to be quoted as $>600V$ for a specified dielectric thickness.
- the effect of water absorption on dielectric strength both before and after refiring.

Dielectric Constant

- measurement of the unit-area capacitance for known thickness of dielectric, for several capacitive structures on the test substrates.
- change of dielectric constant due to the effects of multiple refiring.
- change of dielectric constant as a result of aging.
- measurement of the frequency dependence of the dielectric constant.

Dissipation Factor

- measurement of the variation of dielectric loss (i.e. $\tan \delta$) with frequency.

DISCUSSION

When a number of Integrated-circuit modules are mounted on a single thick-film substrate, the layout of the interconnections usually requires a large number of crossovers. In the design of the layout, conductors which have to pass over each other generally do so orthogonally, and a glass-ceramic dielectric is interposed to provide the physical and electrical isolation required. Generally there is a difference of potential between such conductors as a result of different dc bias levels, and in addition, ac signal voltages may be superimposed on the dc bias. If two conductors should cross orthogonally on either side of a dielectric layer, there may be dc coupling as a result of leakage current through the dielectric and ac coupling as a result of the capacitance. (surface leakage and fringing flux are generally negligible as a result of the layout design)

Several steps can be taken to minimise the effects of this coupling between the circuit layers. Since a glass-ceramic dielectric has distinct mechanical advantages over the glass type, it is to be preferred, but the dielectric constant is higher as a result of the ceramic phase developed. Consequently there is little that can be done to reduce the value of the dielectric constant below about $K = 10$. The common area of the

crossover can be minimised by narrowing the conductors to the practical limit, which is on the order of 0.25mm (= 10mils). For a reasonable yield from the thick-film process, the dielectric is double-printed and fired to a thickness close to 46 microns(= 1.8mils). Although it would be advantageous to increase the thickness, it would be uneconomic for a number of obvious reasons. The coupling capacitance of this minimal sized crossover, assuming that it has a "parallel-plate" structure and that fringing flux can be neglected, is on the order of 0.1pF. Since the reactance above say, 100MHz, is less than $16K\Omega$, it is obvious that many crossovers, in a digital circuit especially, can cause a serious degradation of the circuit performance. Every attempt must be made to minimise the number of crossovers at the design stage, and if this a difficult task, the spacing between conductors carrying digital signals should be increased by alteration of the layout. These comments would apply in the case of VHF analogue signals, and increasing the spacing might prove advantageous if the conductors differed in potential by say, a few hundred volts dc. For a simple crossover, with electrode spacing of about 46microns, the electric field might be close to the dielectric strength under these circumstances. Furthermore, the thick-film conductor compositions all contain a large percentage of Silver, and there is always the risk of migration through the dielectric under high electric fields and humid conditions.

DC Effects

Suppose that a constant dc voltage is suddenly applied across the electrodes of a simple crossover from a highly stabilised low-impedance source. An initial rise in current is observed in the circuit, which subsequently decays to a much lower value after a period of time which usually extends to several seconds, but may amount to one minute or more. If the dielectric strength is not exceeded, the current thereafter remains steady apart from small random fluctuations; if it is exceeded, circuit current continues to increase until the dielectric fails. This behaviour is sketched in Figure 3.

In view of the fact that the thick-film dielectric is a polycrystalline phase embedded in a glass matrix, and most probably includes a number of different kinds of impurity ions trapped at phase boundaries and at lattice imperfections, the response to an electric field at the molecular level will be complex. It is thought that the initial rise in current (as the parasitic capacitance charges) results from bulk transport of impurity ions within the dielectric (leakage current) together with a component of current arising from polarization of the dielectric. (absorption current) The electronic and molecular polarizations would have extremely short relaxation times of about 10^{-13} sec, and the effects would be masked by any orientation, space-charge or ion-jump mechanisms with relaxation times extending to seconds. Dynamic equilibrium is reached

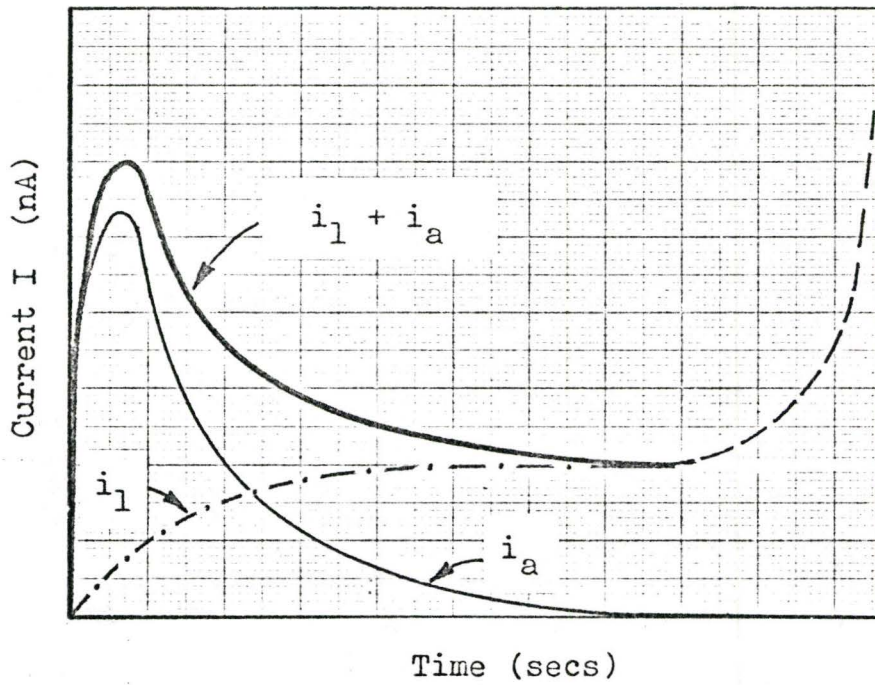


Figure 3. DC response of a crossover dielectric.

i_l = leakage current (conductivity)

i_a = absorption current (relaxation)

----- increase in leakage current
leading to breakdown

between the effects of the electric field, and the randomising effect of the temperature, on the dipoles created. Therefore after a period of time related to the most probable value in the distribution of relaxation times, the absorption current has decayed to a negligible value as the crossover capacitance becomes fully charged. The circuit current at this point in time, neglecting any surface effects, is the value of "leakage" current that should be used to determine the insulation-resistance for the dielectric. In order to make a realistic comparison between different glass-ceramic dielectrics forming crossovers of the same geometry, the thick-film industry adopts the procedure of measuring the insulation resistance after an arbitrarily chosen time lapse of 1min, from the time of application of the dc voltage, for the reason cited above.

It is not always reasonable to neglect surface leakage current, even though every attempt is made in the design of a crossover to minimise it. For example, the dielectric is made to overlap the common area associated with the upper and lower conductors by a margin which makes any possible surface leakage path at least an order of magnitude greater than the dielectric thickness. The effect of surface leakage leads to a pessimistic value for the insulation resistance, and its presence can be inferred from a repeat measurement of the latter after drying and coating with an encapsulant which is impervious to water. The mobility of various impurity ions which become attached to the dielectric surface during processing, increases with the

presence of a film of moisture, and if in addition a dc voltage is present between the electrodes, there is the risk of Silver ion migration and dendritic growth at the cathode if the dielectric happens to be porous.

Dielectric strength is defined as the maximum voltage-gradient which a material can withstand before a catastrophic failure occurs, and is generally obtained from the results of many destructive tests carried out under carefully controlled conditions. Thick-film dielectrics are never exposed to such high electric fields that there is the risk of this kind of breakdown, and a more meaningful test has been devised which indicates the degree of degradation resulting from a substantial increase in the applied electric field, without initiating the breakdown. In this test, the insulation resistance is measured under the conditions outlined earlier, at a voltage of 100V dc; a repeat measurement is made at, say, 500V dc. If the insulation resistance has not decreased by more than 3 orders-of-magnitude relative to that at 100V, then this "operational" definition of dielectric strength is quoted as >500V for a dielectric film of specified thickness.

The breakdown mechanism for commercial dielectrics of the glass-ceramic type is probably initiated by electrons from impurity atoms and aided by the release of ions from phase boundaries and structural defects as the electric field is increased.

The printed thick-film is likely to have a distribution of various imperfections on a macroscopic scale, and the fired film will be inhomogeneous; arcing at voids within the structure, as a result of the non-uniform electric field, causes localised melting and chemical change. If this is severe it is likely that a conducting path will develop as a result of metallic diffusion into the dielectric, and the crossover breaks down. At this stage, the damage is permanent.

It often happens that if a crossover is tested immediately after processing it will be found to have a short-circuit, probably as a result of some diffusion of metallic ions from the conductor composition through the common glass phase of the structure, during the growth of the ceramic phase within the dielectric. The process of deliberately refiring can sometimes remove this conductive path permanently, and the crossover has as high an insulation resistance as one which did not have a short circuit initially. In some cases, the short can be removed by the application of a dc electric field somewhat lower than the dielectric strength of similar structures. The mechanism is probably due to impurity atoms which have become trapped during the devitrification at phase boundaries, and are released by subsequent heat treatment or the application of a high electric field. By the same token, it may be possible to remove one shorting path, only to replace it by another, and unfortunately this seems to be the case. However, since there is nothing to be lost from an Engineering

viewpoint, it is worth the risk to obtain a higher yield, and it is not uncommon for other kinds of dielectric used in Electrical Engineering to be "conditioned" with an electric field before testing in their intended environment.

AC Effects

When an ac voltage is applied to a crossover, the only polarization mechanisms which can contribute to the permittivity of the dielectric are those whose range of relaxation times lie below the period of oscillation of the ac electric field. Therefore in the frequency range 60Hz - 100MHz for example, the total polarizability is due to the sum total of all the polarizing mechanisms mentioned previously. Although it might be expected that the permittivity decreases as the frequency increases because of the progressively smaller contribution from space-charge and ion-jump polarizations, this does not appear in the results for glass-ceramic crossovers. In the region of 20MHz there is a noticeable increase in permittivity which might be attributable to vibration loss for the various ions in the glass phase. In such a complex system as a thick-film dielectric, it is almost impossible to be specific, and for most Engineering purposes it is more meaningful to model the behaviour with an equivalent circuit, whose component values are chosen to match the empirical results as far as possible.

Similar comments apply to the consideration of dielectric

loss which is generally characterised by a measurement of the loss-tangent, $\tan \delta$. The dielectric loss of glass-ceramics is thought to be due to ion-jump relaxation in the glass phase at electrical frequencies of practical interest, the contribution due to dc conductivity being negligible at normal ambient temperatures. Whereas at dc the loss is described in terms of the leakage current, at ac there is the combined effect of leakage and absorption currents, with the latter being the dominant term. There is a general tendency for the dielectric loss to decrease with increasing frequency until the vibration losses mentioned earlier begin to dominate and the dielectric loss increases again. Part of this effect would be due to the increase in effective series resistance of the crossover structure as a result of the skin effect at frequencies high enough that only part of the conductor layer is effective.

Circuit model for Crossovers and Printed Capacitors

A number of network-analysis computer programs exist for the evaluation of the circuit performance of specific components when interconnected; the physical layout of such components can influence the behaviour of the complete circuit even though the electrical interconnections are the same in each case. The computer programs require suitable models for each of the circuit components, which, in the case of thick-film networks, includes crossovers. The distributed nature of thick-film components tends to lead to complex lumped-element

models, especially at frequencies in the Gigahertz range, but in the case of a single printed crossover the model shown in Figure 4 is adequate.

The resistor R_s represents the resistance of the leads, electrodes and electrode/dielectric interfaces of the crossover. The inductive effect of the parasitic capacitance C_x at very high frequencies where it becomes significant, together with any lead inductance, is lumped into the inductor element L . The resistor R_p represents the insulation resistance at dc, and both polarization and leakage losses under ac conditions. The limitations of such a model centre on the fact that the model parameters are frequency, humidity and temperature dependent, and must be measured in the ranges of interest. Obviously, if the frequency range of interest is severely restricted, then the model is easily simplified to a parallel equivalent at low frequency or a series equivalent at high frequency. In view of the fact that the Q-meter is a convenient instrument with which to measure the model parameters in terms of an equivalent parallel branch, there is good reason for favouring this choice at all frequencies, performing the parallel→series transformation as required.

With reference to Figure 4, the admittance of the network can be written,

$$Y = \frac{1 + j\omega C_x R_p}{(R_s + R_p - \omega^2 L C_x R_p) + j\omega(L + C_x R_s R_p)} \quad (1)$$

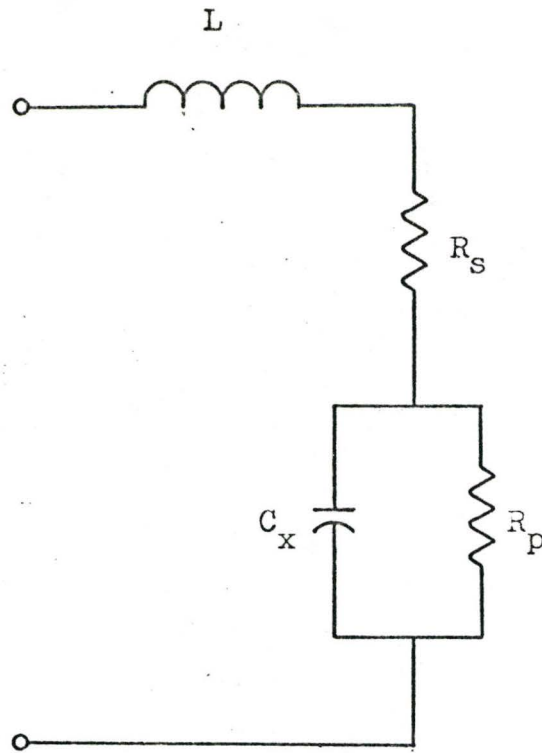


Figure 4. Equivalent circuit-model for a printed crossover.

L = lead and capacitor inductance

R_s = resistance of leads, electrodes and electrode/
dielectric interfaces

R_p = representation of polarization loss and
insulation resistance (leakage)

C_x = parasitic capacitance of crossover

and after rationalising the expression can be rearranged into the form,

$$Y = G + jB_c$$

where:

$$G = \frac{R_p + R_s [1 + (\omega C_x R_p)^2]}{(R_s + R_p - \omega^2 L C_x R_p)^2 + \omega^2 (L + C_x R_s R_p)^2} \quad (2)$$

and

$$B_c = \frac{\omega [C_x R_p^2 - L \{1 + (\omega C_x R_p)^2\}]}{(R_s + R_p - \omega^2 L C_x R_p)^2 + \omega^2 (L + C_x R_s R_p)^2} \quad (3)$$

In (2) and (3), G and B_c are the conductance and capacitive susceptance respectively of an equivalent parallel R,C network. The Q-meter is used to determine the values of R and C as described in the Appendix.

From the ratio of the expressions given in (2) and (3), the loss tangent can be calculated:

$$\text{Tan } \delta = \frac{R_p + R_s [1 + (\omega C_x R_p)^2]}{\omega [C_x R_p^2 - L \{1 + (\omega C_x R_p)^2\}]} \quad (4)$$

At frequencies for which L is insignificant compared with the effects of the remaining parameters, equation (4) can be simplified to the form:

$$\text{Tan } \delta \approx \frac{1}{\omega C_x R_p} + \omega C_x R_s \quad (5)$$

It can be easily shown that for typical values of R_p , R_s and C_x for thick-film crossovers, the value of equivalent parallel capacitance, C , as measured by the Q-meter, is equal to the model parameter C_x for all electrical frequencies of interest. Similarly, the equivalent parallel resistance, R , is equal to model parameter R_p (to within approximately 4%) for frequencies below about 500kHz. For frequencies above 500kHz, the relationship between R and R_p should be obtained from the expression:

$$R \approx \frac{R_p}{1 + \omega^2 C_x^2 R_s R_p} \quad (6)$$

The value for R_s can be obtained from a measurement of $\tan \delta$ at sufficiently high frequency ($>5\text{MHz}$) that the second term in equation (5) is the dominant one.

It can be shown that the measured value of $\tan \delta$ ($=1/\omega CR$) is equal to the value of $\tan \delta$ predicted from equation (5) for the model, at all electrical frequencies of interest for the practical application of thick-film technology.

A comparison of model behaviour and measurements for capacitor pad E (Figure 2) is given on the graph of Figure 28 for System 'A', by way of example. The values of the parameters were $C_x = 80\text{pF}$, $R_s = 0.24$ ohms and $R_p = 10$ Megohms.

Such a relatively simple model as that of Figure 4 cannot predict peaks due to resonance loss which might occur in the electrical frequency band for thick-film dielectrics.

PROCEDURE

Identification of Materials and Test Substrates

For the purposes of this report, two compatible paste systems from different Suppliers were selected, and identified as System 'A' and System 'B' for proprietary reasons. Each system comprises one Platinum-Silver conductor paste and one glass-ceramic dielectric paste.

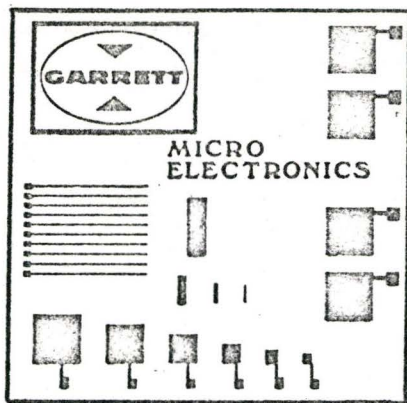
Printed substrates prepared from System 'A' materials consist of a set of 2" x 2" alumina substrates coded $A_1, A_2 \dots \dots A_{10}$ utilising the entire test pattern illustrated in Figure 2, and a set of 1" x 1" alumina substrates coded $A_{11}, A_{12} \dots \dots A_{30}$ utilising only the array of crossovers, the remainder of the pattern being blanked off. For System 'B' materials only one set of 2" x 2" alumina substrates were prepared because of the limited manufacturing variations that proved feasible for this system. They were coded $B_1, B_2 \dots \dots B_{20}$ and utilised the entire test pattern.

Choice of Test Pattern and Screen Preparation

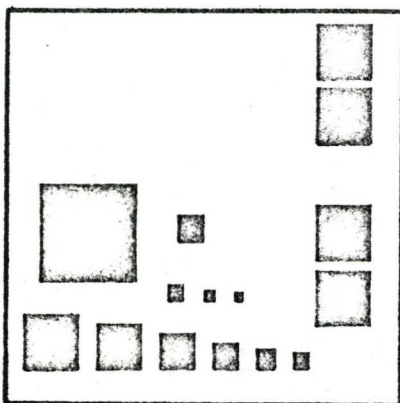
The test pattern used in this evaluation was selected on the basis that the test structures would be typical of the range to be found in the kind of thick-film circuits currently manufactured with other types of paste at Garrett Manufacturing.

In order to process the test pattern, which is illustrated in Figure 2, three stencil screens were prepared; each one contains a separate pattern corresponding to the base electrodes, the dielectric layer, and the counter-electrodes respectively. The positive film masters used to generate these stencil screens are illustrated in Figure 5.

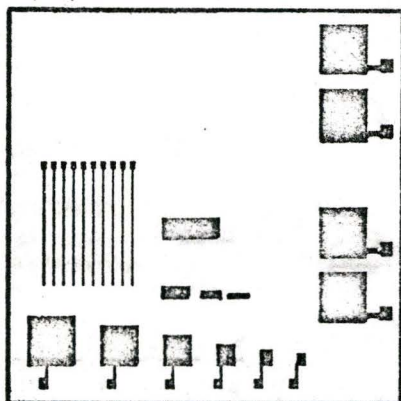
Three '200-mesh' screens were assembled to their support frames and tensioned so that the measured deflection at the centre of the screen was 1.0 ± 0.1 mm when a 0.5kg load was applied. In a clean-room under amber lighting, the screens were cleaned with detergent and isopropyl alcohol. A piece of 'Autoline' film was applied to the underside of the mesh, and attached to it by means of a layer of 'Encolsol' emulsion applied by squeegee from the opposite side. After drying, the backing was removed from the film, and each of the three screens was placed in contact with its appropriate positive film master in a vacuum exposure frame. Exposure to UV light for 7 minutes is followed by a wash in hot water spray (40°C) which removes the emulsion which was protected from exposure by the film master, leaving a negative screen pattern. After drying, any areas at the perimeter of the pattern are blocked-out to prevent paste leakage when the screen is used to print the desired pattern on to a suitable alumina substrate.



(a) Base Electrodes



(b) Dielectric Layer



(c) Counter-electrodes

Figure 5. Positive film masters.

Screen-printing and Firing of Test Substrates

A standard Fresco screen printer was used throughout the evaluation. Each screen was set-up in the printer to give a 0.030" snap-back, and sufficient pressure applied to the black-rubber squeegee for the pattern to print clearly when the appropriate paste was applied to the upper surface of the screen. (The 'snap-back' is the vertical deflection caused by the motion of the squeegee, to bring the screen into line-contact with the substrate beneath the squeegee as the print is made.) Pre-fired and cleaned 96% Alumina substrates were placed in turn on the substrate-holder of the printer, and the alignment between screen pattern and substrate checked by making a number of trials to ensure adequate paste loading of the screen apertures and clean-edged prints. The freshly-printed test substrates were inspected, placed in a dust-free cabinet to allow time for the screen-impression marks to disappear, and subsequently oven-dried for 12 minutes at 150°C. Each test substrate was then fired according to the temperature profile illustrated in Figure 1, although the sequence of printing, drying and firing was varied according to the schedule illustrated in Figure 6. This schedule was adopted because the first part of the evaluation involved identifying the best manufacturing sequence from a number of possible alternatives, and seeing if there was any correlation between the sequence chosen and the yield obtained in terms of the percentage of good crossovers.

OPTION 1(a)

Print, dry, fire
Base conductor
↓
Print, dry 1st
Dielectric layer
↓
Print, dry 2nd
Dielectric layer
↓
Print, dry
Counter-electrode
↓
Co-fire dielectric
with
Counter-electrode

OPTION 1(b)

Fire double-printed
Dielectric layer
↓
Print, dry
Counter-electrode
↓
Fire
Counter-electrode

OPTION 2(a)

Print, dry, fire
Base conductor
↓
Print, dry, fire
1st Dielectric
layer
↓
Print, dry 2nd
Dielectric layer
↓
Print, dry
Counter-electrode
↓
Co-fire 2nd dielectric
with
Counter-electrode

OPTION 2(b)

Fire 2nd
Dielectric layer
↓
Print, dry
Counter-electrode
↓
Fire
Counter-electrode

Figure 6. Processing sequences.

With reference to Figure 6, Options 1(a) and 2(a) involve a co-firing procedure for the second dielectric layer and counter-electrode; these Options differ in that the first dielectric is only dried in 1(a) whereas it is fired first in 2(a). As far as Options 1(b) and 2(b) are concerned, all layers are fired separately, but in 1(b) the dielectric is printed double before firing whereas in 2(b), each of the dielectric prints is fired individually. The number of individual processing steps is least for Option 1(a) and most for 2(b).

All dried prints were subjected to an identical temperature profile during the firing operations, and after being allowed to cool to room temperature, the thickness of successive prints was measured with a Zeiss light-section microscope to maintain process control. Average values of the thickness of fired prints are shown on the cross-sectional view of a typical crossover given in Figure 7.

Table 2. illustrates how each substrate was processed using both System 'A' and System 'B' materials. Note that System 'B' materials could not be processed using either of the co-firing Options, 1(a) and 2(a), without the counter-electrode becoming detached from the dielectric on cooling. The test substrates made using this sequence were discarded.

Sequence of Measurements

The measurements made on the test substrates were

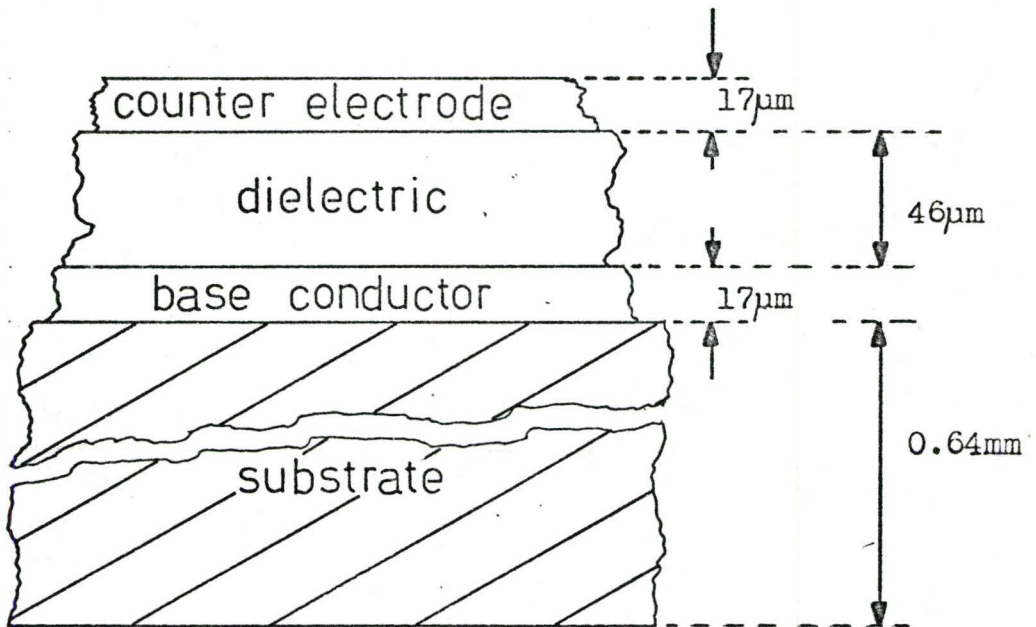


Figure 7. Cross-section through a printed crossover.

Option	Substrate Code-number	
	System 'A'	System 'B'
1(a)	A ₂ , A ₆ , A ₁₀ and A ₂₁ to A ₃₀	—
1(b)	A ₄ , A ₈	B ₁₁ to B ₂₀
2(a)	A ₁ , A ₅ , A ₉ and A ₁₁ to A ₂₀	—
2(b)	A ₃ , A ₇	B ₁ to B ₁₀

Table 2. Substrate code-numbers for processing options.

substantially the same for both systems, and for convenience were divided into several parts:

- Part 1. Identification of the number and location of short-circuited crossovers on the printed 'array' of each substrate. This was carried out using an RCA Volt-Ohmyst Model WV-77E multimeter (1000M Ω range), and measuring the resistance between each upper and lower electrode-pair for the 100 crossovers in the array.
- Part 2. A repeat of Part 1. after selected samples had been subjected to successive thermal shocks by re-firing several times at the 850 $^{\circ}$ C peak temperature profile.
- Part 3. Measurement of the Insulation resistance presented by a number (generally 100) of crossovers connected in parallel, at various levels of dc bias voltage. The equipment is indicated in Figure 8.
- Part 4. Determination of Dielectric Strength (as defined under the 'operational definition' described in the INTRODUCTION).
- Part 5. Measurement of Insulation resistance variation as a result of water absorption from a single drop of deI water placed directly in contact with the counter-electrode and surrounding dielectric of each crossover.

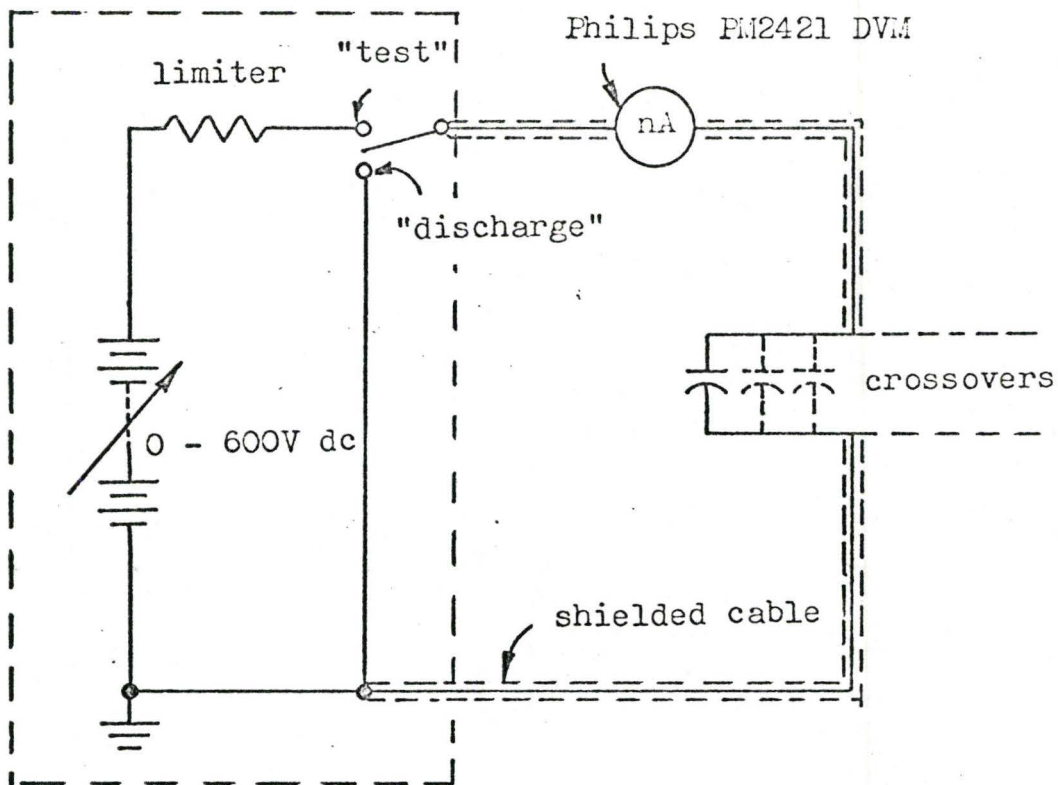


Figure 8. Measurement of leakage current.

- Part 6. A repeat of Parts 3, 4 & 5, after selected samples had been subjected to thermal shocks by refiring several times.
- Part 7. Measurement of the unit-area capacitance using larger crossovers of varying area on the substrates, and determination of the Dielectric constant at 1MHz and 22°C., for structures of known geometry.
- Part 8. A repeat of Part 7. after a time-lapse of 3 months, for test substrates stored at a room ambient temperature of 22°C, to investigate the effects of aging.
- Part 9. A repeat of Part 7. after selected samples had been re-fired once.
- Part 10. Measurement of the variation in Dielectric constant as a function of frequency, using a Marconi Model TF 1245A Q-meter.
- Part 11. Measurement of the variation in Dissipation factor, $\tan \delta$, as a function of frequency using the Q-meter.

RESULTS

Part 1.

Each of the test substrates processed according to the four options available for System 'A' materials was examined for short-circuited crossovers and capacitors. The results are illustrated in Figures 9 and 10. Figure 9 is a representation of the array of crossovers for each substrate, on which a black dot signifies a short-circuit. The same procedure is used in Figure 10, which presents the information in tabular form for the remaining structures on the test substrates.

A trial run for System 'B' materials had shown that co-firing of the counter-electrode was not feasible. Consequently only Options 1(b) and 2(b) were employed, and the results are presented as for System 'A' in Figures 11 and 12.

There does not appear to be any fault on the active areas of the mesh screens, such as a particle of foreign matter embedded in the mesh, because this would be indicated by a short-circuit consistently appearing at the same location. This does not seem to be the case for the batch of test substrates used in this evaluation.

A summary of the yield figures for both systems of materials follows Figure 12. The 'sample size' is taken to be

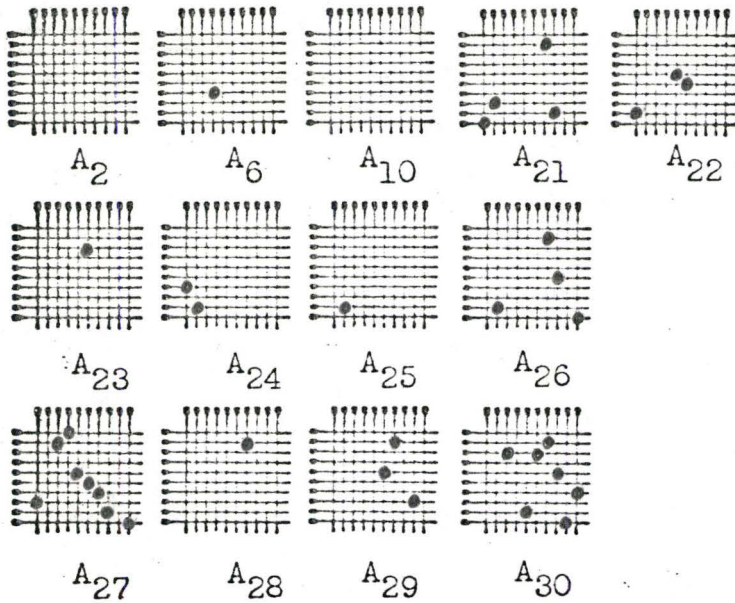
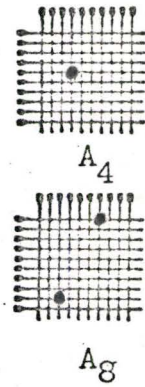
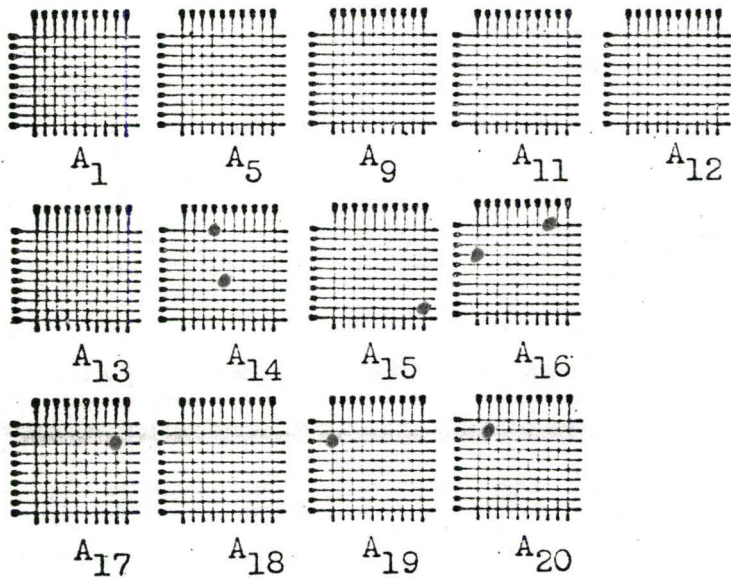
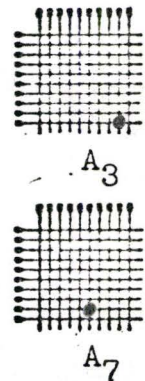
OPTION 1(a)OPTION 1(b)OPTION 2(a)OPTION 2(b)

Figure 9. Location of short-circuits on arrays processed with System 'A' materials.

Process	Option 1(a)	Option 1(b)	Option 2(a)	Option 2(b)
Substrate	A ₂ A ₆ A ₁₀	A ₄ A ₈	A ₁ A ₅ A ₉	A ₃ A ₇
Capacitor				
A				
B				
C				
D				
E				
F				
G				
H				
I				
J				
Crossover				
K				
L				
M				
N				

Figure 10. Location of short-circuits on crossovers/capacitors for System 'A'.

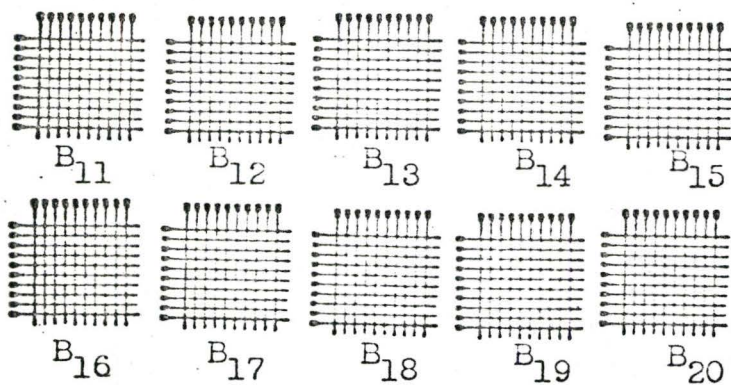
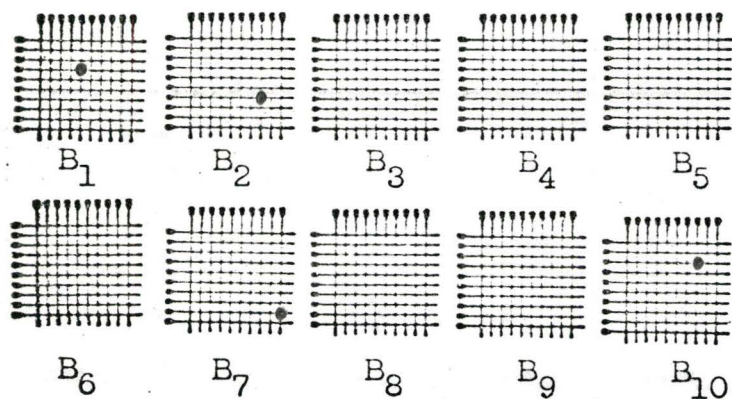
OPTION 1(b)OPTION 2(b)

Figure 11. Location of short-circuits on arrays processed with System 'B' materials.

Process	Option 1(b)	Option 2(b)
Substrate	B ₁₁ B ₁₂ B ₁₃ B ₁₄ B ₁₅ B ₁₆ B ₁₇ B ₁₈ B ₁₉ B ₂₀	B ₁ B ₂ B ₃ B ₄ B ₅ B ₆ B ₇ B ₈ B ₉ B ₁₀
Capacitor		
A		•
B		•
C	•	
D		
E	•	•
F		•
G	•	
H		
I		•
J		
Crossover		
K		•
L		
M		
N		•

Figure 12. Location of short-circuits on crossovers/capacitors for System 'B'.

the total number of crossovers within a batch of test substrates for each processing Option:

<u>System 'A'</u>			
	<u>Option</u>	<u>Sample size</u>	<u>Yield (%)</u>
Arrays	1(a)	1300	97.3
	1(b)	200	98.5
	2(a)	1300	99.4
	2(b)	200	99.0
Capacitors & Crossovers	1(a)	42	97.6
	1(b)	28	96.4
	2(a)	42	100
	2(b)	28	100

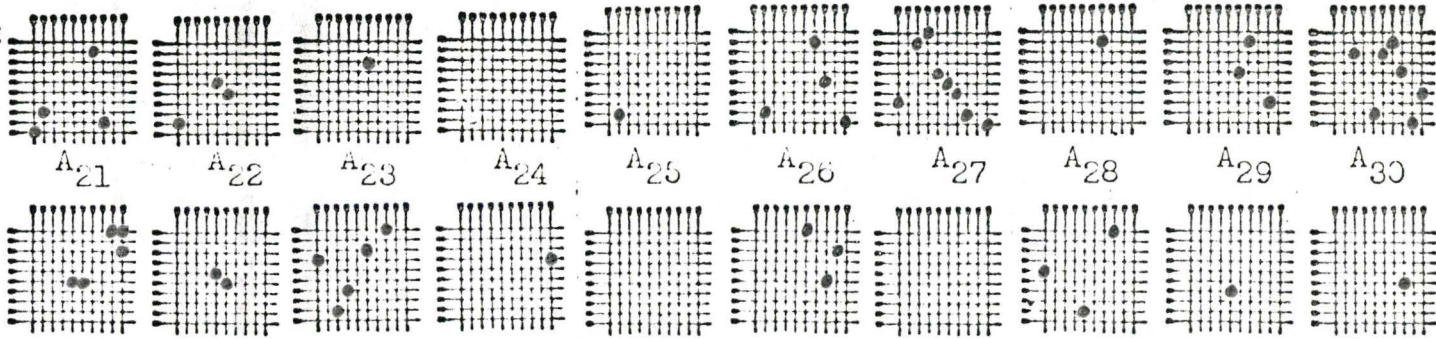
<u>System 'B'</u>			
Arrays	1(b)	1000	100
	2(b)	1000	99.6
Capacitors & Crossovers	1(b)	140	95.7
	2(b)	140	93.6

Part 2.

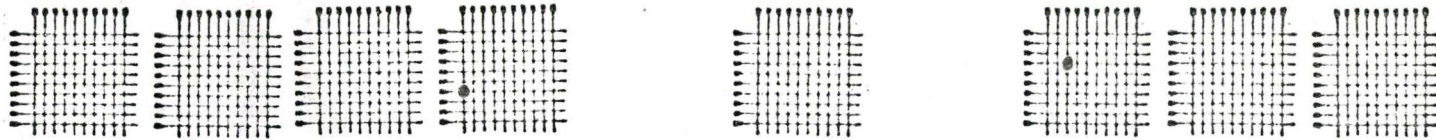
The results of the effect of re-firing on selected test substrates from each batch are illustrated in Figures 13 and 14 for System 'A' materials, and Figures 15 and 16 for System 'B' materials. A summary of the yield figures for both systems follows Figure 16:

OPTION 1(a)

After processing



After re-firing once



After re-firing three times

Figure 13. Effect of re-firing for System 'A'.(Option 1(a))

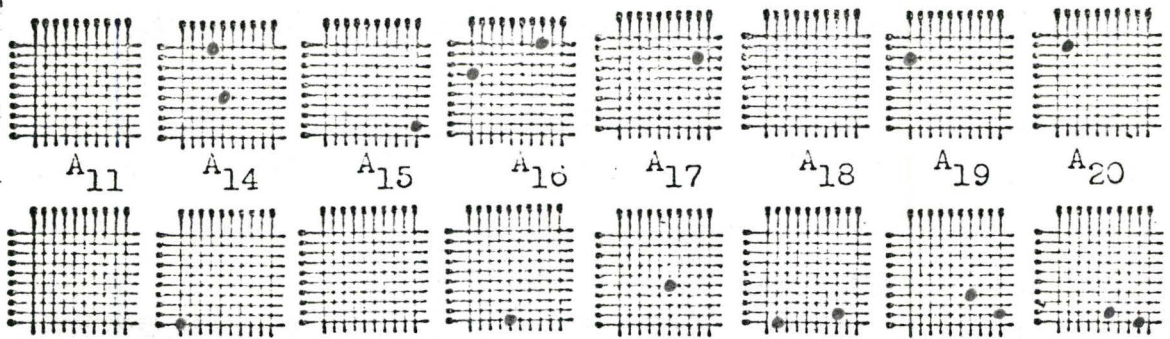
OPTION 2(a)After processingAfter re-firing once

Figure 14. Effect of re-firing for System 'A'.(Option 2(a))

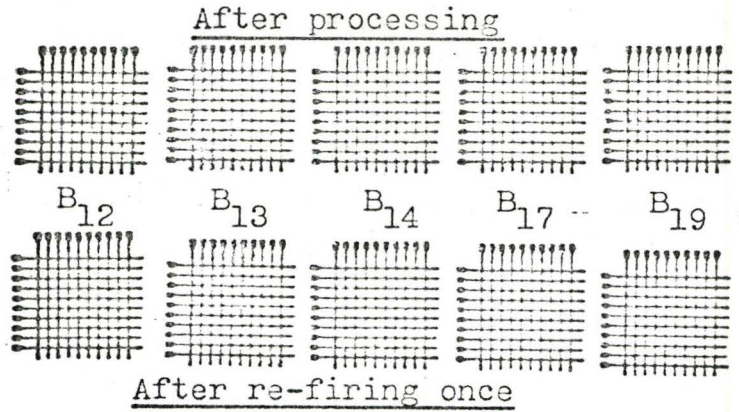
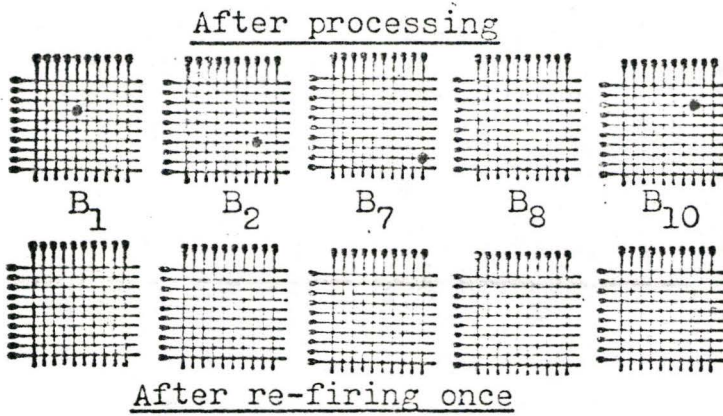
OPTION 1(b)OPTION 2(b)

Figure 15. Effect of re-firing on arrays processed with System 'B' materials.

Process	Option 1(b)	Option 2(b)
Substrate	B ₁₂ B ₁₃ B ₁₄ B ₁₇ B ₁₉	B ₁ B ₂ B ₇ B ₈ B ₁₀
Capacitor		
A	•	
B	•	
C		• •
D		•
E	•	•
F		
G	•	
H		
I		•
J		
Crossover		
K		
L		
M		
N		•

Figure 16. Effect of re-firing on crossovers/capacitors for System 'B'.

<u>System 'A'</u>	<u>Yield(%)</u>	
	<u>Option 1(a)</u>	<u>Option 2(a)</u>
After processing:	96.6	99.0
After re-firing once:	97.9	98.9
After re-firing 3 times:	99.7	-

<u>System 'B'</u>	<u>Yield(%)</u>	
<u>Arrays</u>	<u>Option 1(b)</u>	<u>Option 2(b)</u>
After processing:	100	100
After re-firing once:	99.2	100
<u>Capacitors & crossovers</u>		
After processing:	91.4	87.1
After re-firing once:	88.6	90.0

Part 3.

Selected substrates from each system were prepared for the insulation resistance tests by connecting in parallel, the set of 100 crossovers on the array for each substrate.

The network so formed was used in the set-up shown in Figure 8, and the leakage current for the parallel set of crossovers was measured as a function of the dc voltage applied. The behaviour of a typical single crossover under normal (i.e. 'dry') conditions is illustrated for two different test substrates from System 'A', in the curves appropriately labelled in Figure 17. The corresponding behaviour for

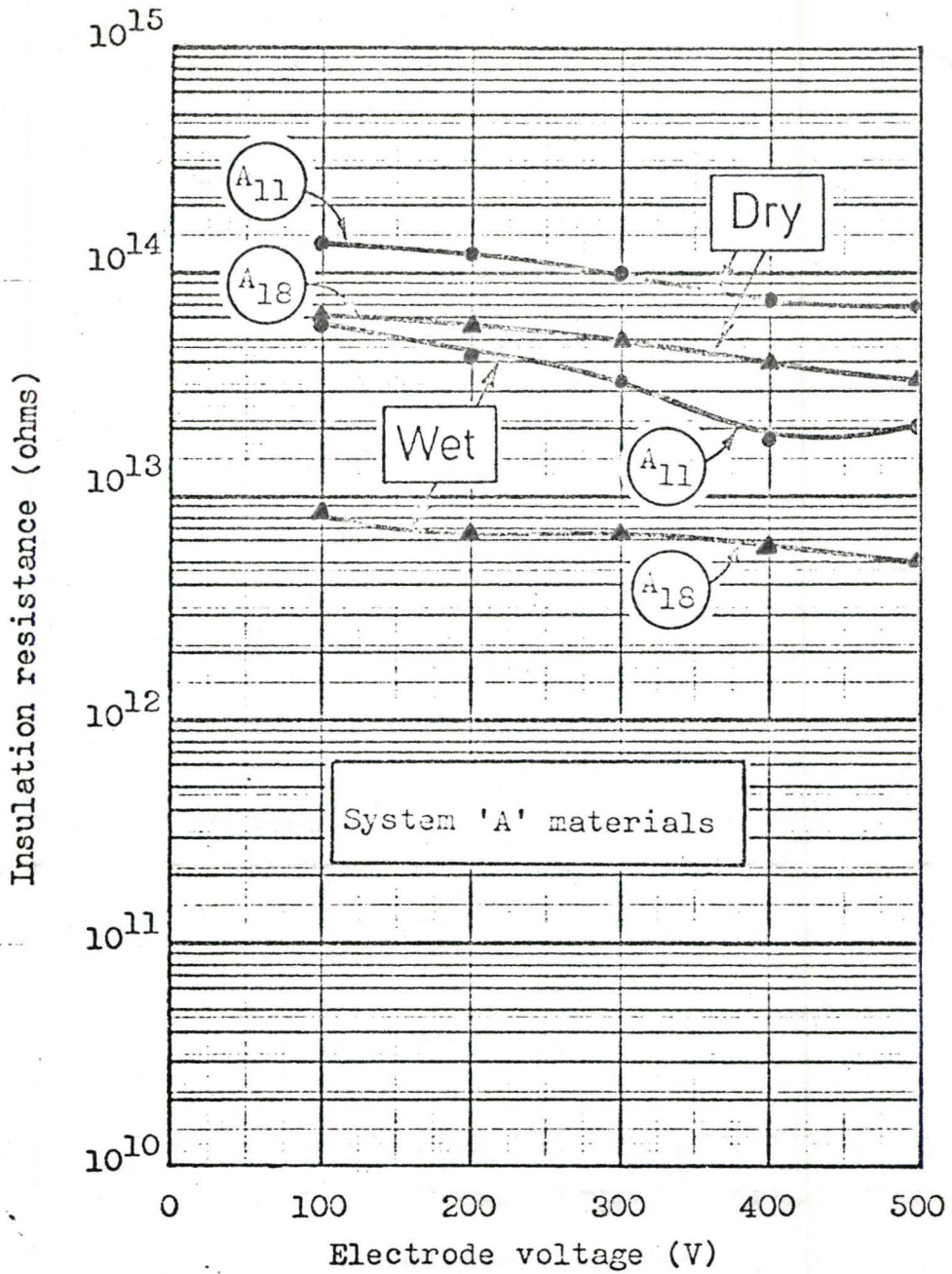


Figure 17. Effect of water absorption on insulation resistance.

five different test substrates from System 'B' is illustrated in Figure 18.

The difference in behaviour of the two systems is quite apparent. Neither of the samples for System 'A' suffered breakdown and the insulation resistance decreased only slightly between 100V and 500V dc, maintaining a value greater than 3×10^{13} ohms. However, for System 'B', three out of five samples suffered breakdown at voltages less than 150V dc, and all showed substantial decreases in insulation resistance to values as low as 2 Megohms.

Part 4.

The tests for dielectric strength under the conditions described in the 'operational definition' quoted previously, were made as follows:

Single crossovers on the arrays of test substrates from System 'A' were connected to the equipment shown in Figure 8, and 100V dc applied; the voltage was increased to 600V dc, and the decrease in insulation resistance was noted. The results for each test substrate are displayed on the chart of Figure 20(a), in which the upper bar denotes the insulation resistance at 100V dc and the lower bar, the value at 600V dc. In every case, the reduction in insulation resistance was less than an order of magnitude.

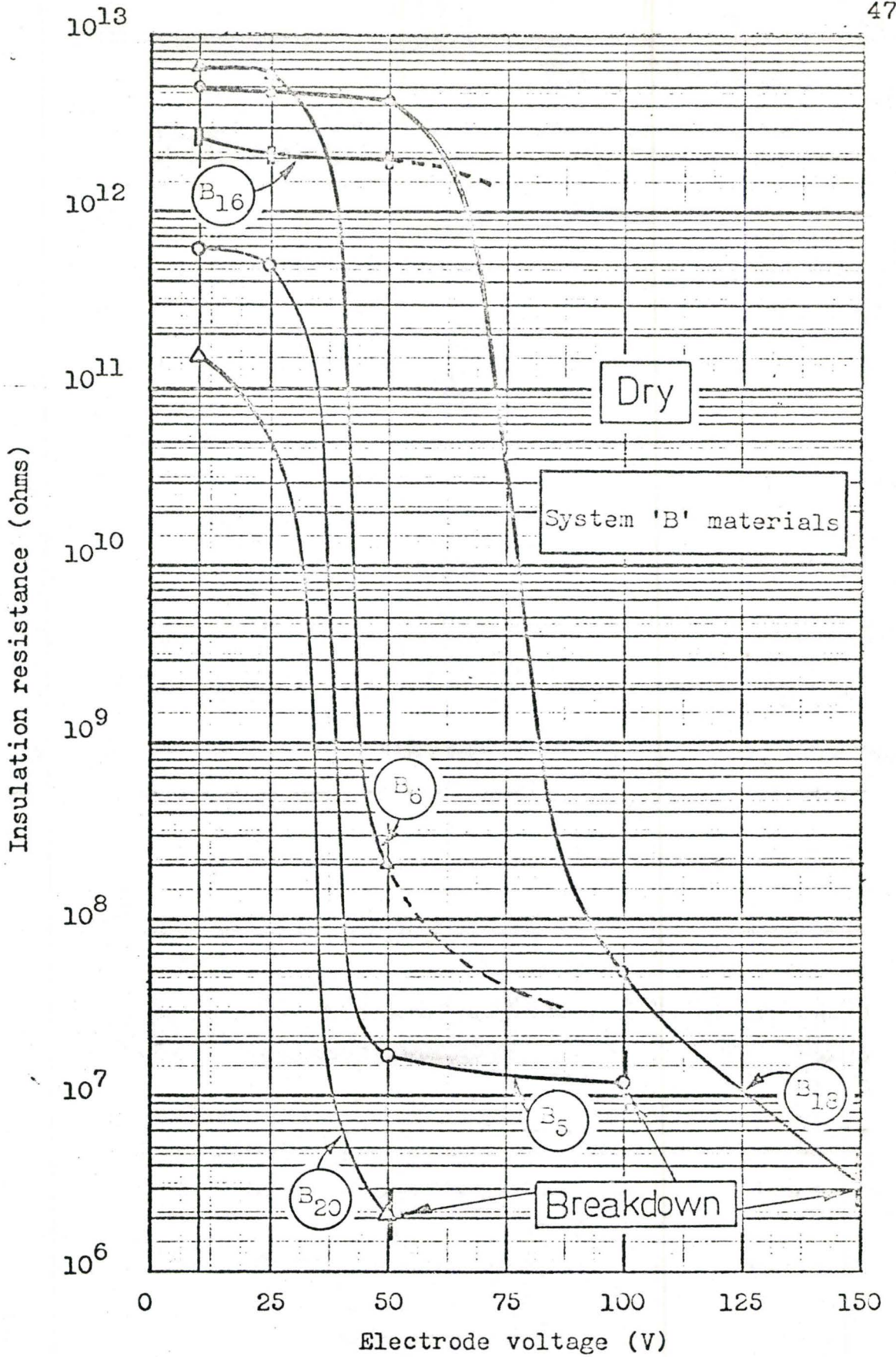


Figure 18. Insulation resistance.

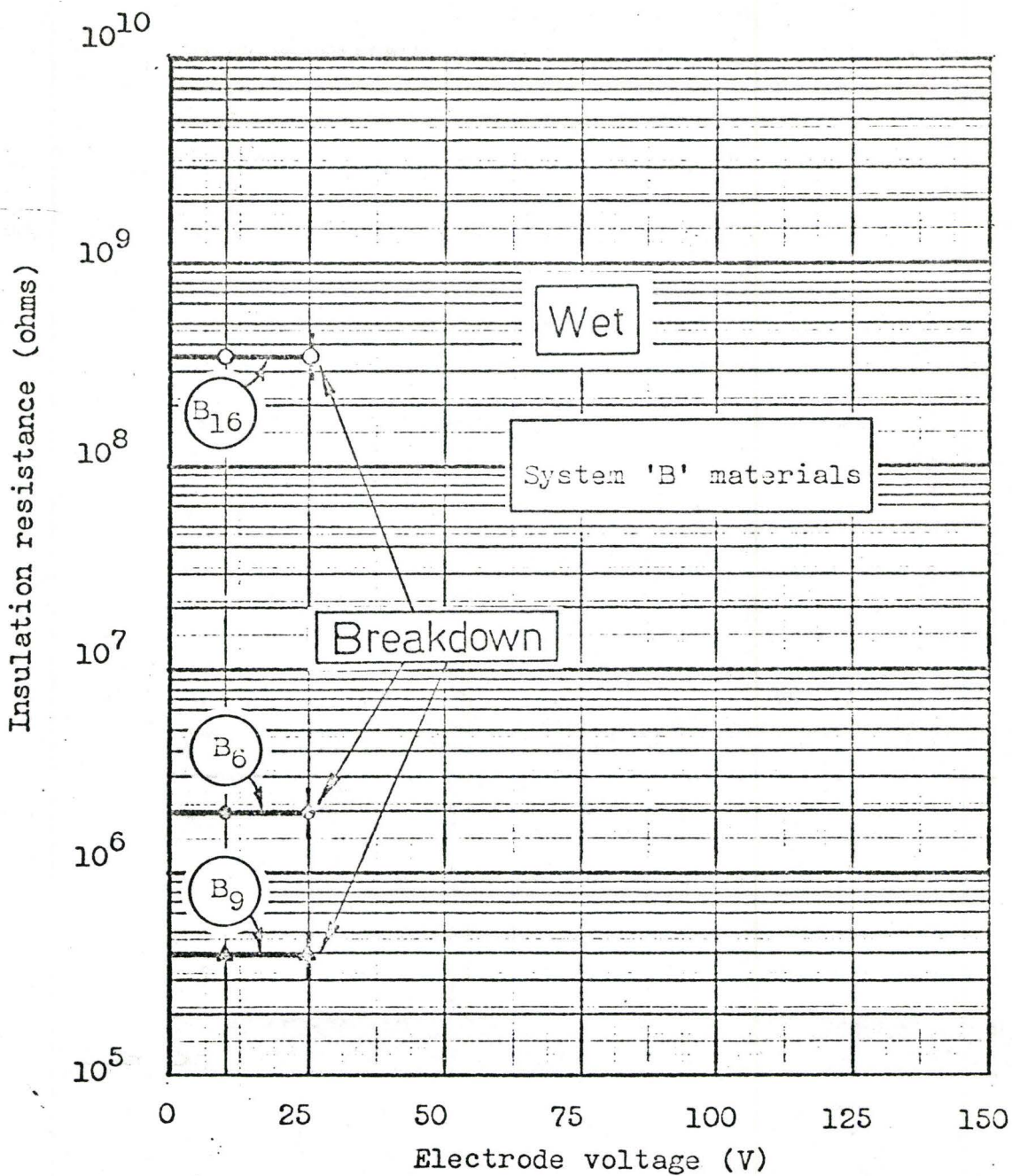


Figure 19. Effect of water absorption on insulation resistance. (dry test conditions-- see Figure 18.)

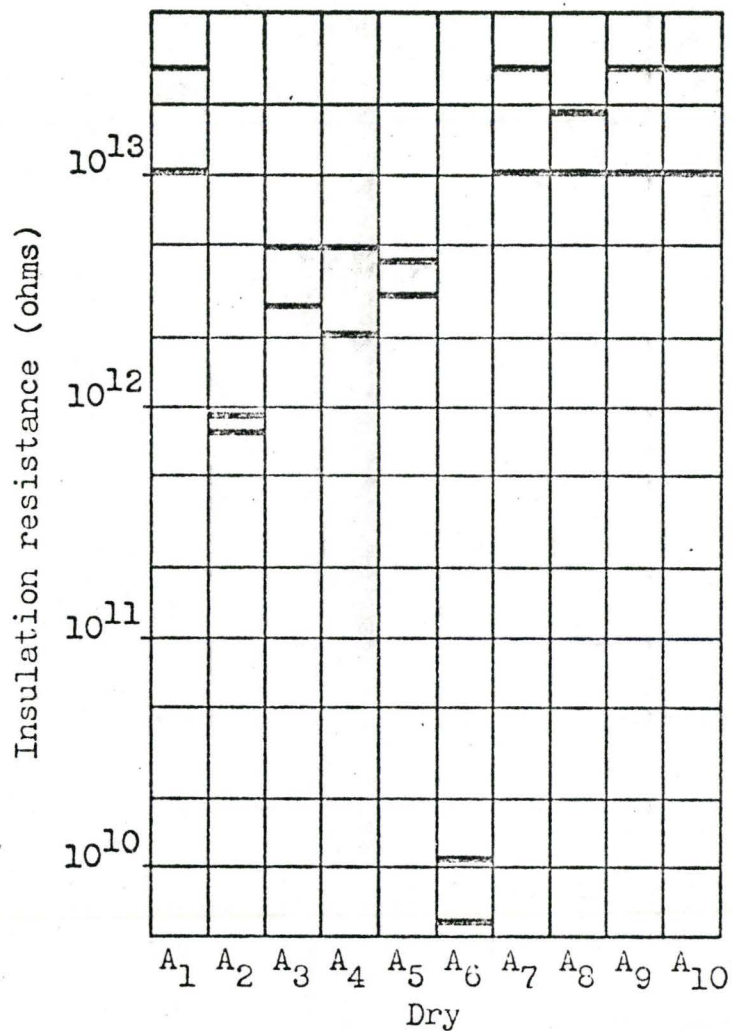


Figure 20(a)

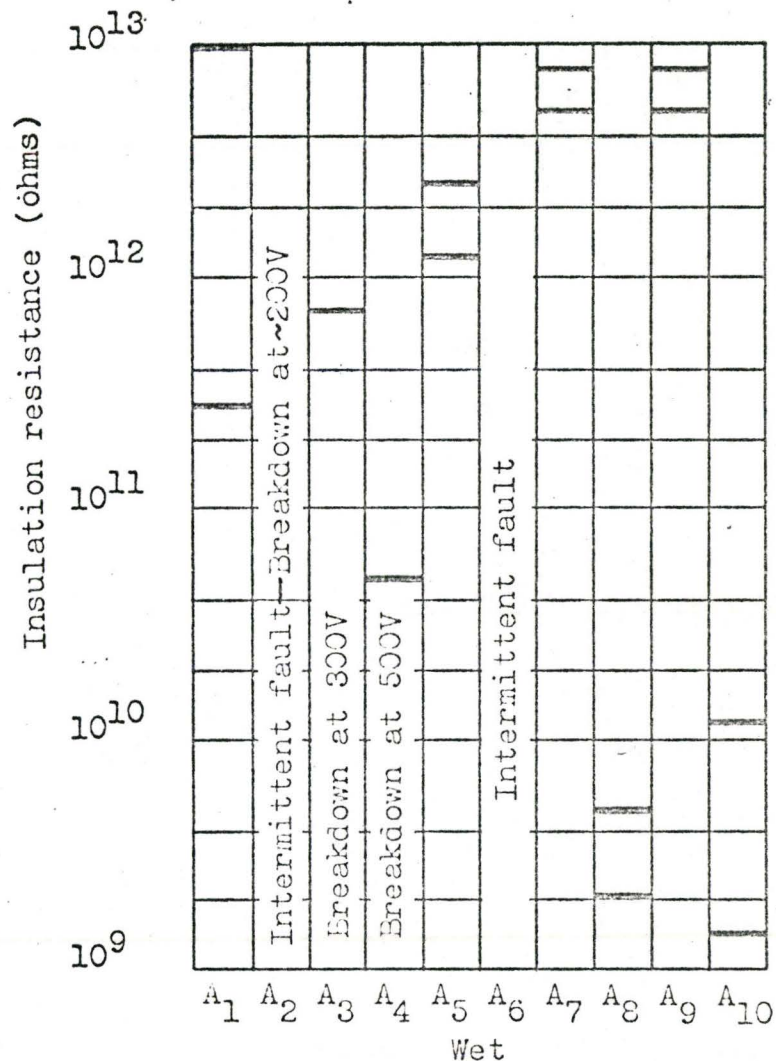


Figure 20(b)

100/600V dc dielectric strength test results.

Part 5.

In this part of the experiment, the test is conducted as in part 3, but the effect of water absorption by the dielectric is examined by placing a single drop of deI water directly in contact with the counter-electrode and surrounding dielectric of the crossover being tested. (This procedure, which is far more severe than similar kinds of tests conducted in humidity chambers at the same temperature, is referred to as the 'water-drop' test in thick-film literature.)

The results for System 'A' are given in the graph of Figure 17 for 100 paralleled crossovers with a widely spread water-drop to cover all counter-electrodes, and the insulation resistance plotted on the basis of a single crossover; in the chart of Figure 20(b), the results are for a water-drop placed over a single crossover, with the test procedure being the same as for part 4.

The results for System 'B' are given in Figure 19, the test condition being for 100 paralleled crossovers as described for System 'A' above. Obviously, the dielectric strength test for System 'B' could not be made.

Summarising the results for System 'A', at the same voltage level as the dry condition, the insulation resistance is decreased by less than an order of magnitude in all but one sample, and of those that did not display any erratic

behaviour, a voltage of at least 200V dc could be sustained without the insulation resistance falling below 10^9 ohms for all the samples tested.

For System 'B', the numerical results are disconcerting; all three samples suffered breakdown as low as 25V dc, and in the worst case, the insulation resistance had fallen as low as 4×10^5 ohms. In general terms, one could say that System 'A' was better than System 'B' by four orders of magnitude in insulation resistance, and an order of magnitude in dielectric strength.

Part 6.

The effect of re-firing on the insulation resistance values for samples from System 'A' test substrates, was examined for both dry and wet conditions, and the results are given in Figures 21, 22 and 23.

Comparison between Figures 17 and 21 shows that re-firing once did not have a significant effect on the insulation resistance of the sample, other than a greater rate of decrease in value with increasing applied dc voltage. Similarly, the results for the water-drop test do not differ significantly whether the sample has been re-fired once or not, and the insulation resistance remained above 10^{12} ohms for both samples.

Two test substrates, A₁₅ and A₂₅, were chosen as samples because they each had one short circuit on their

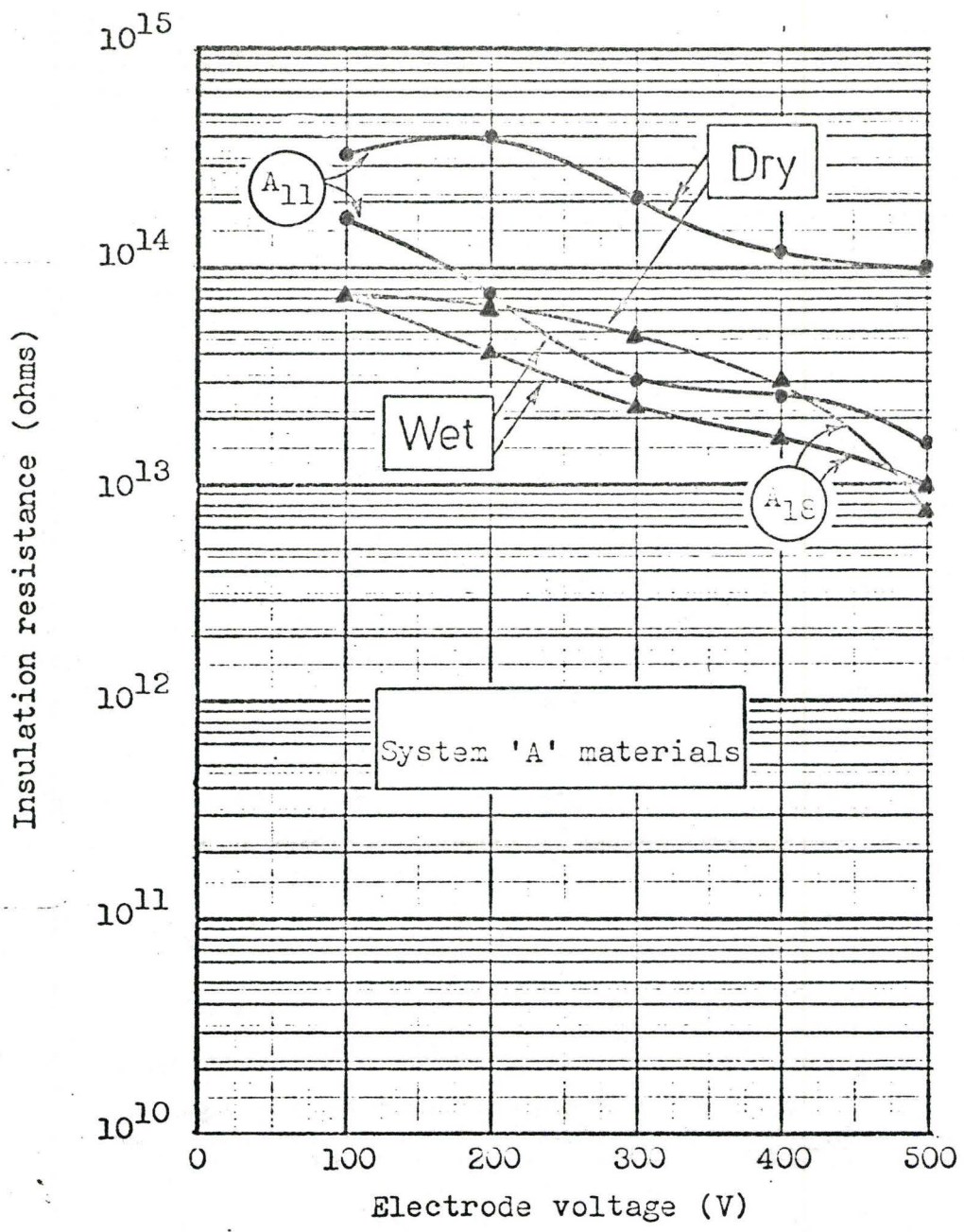


Figure 21. Effects of re-firing once on insulation resistance.

arrays after processing, and both short-circuits disappeared after re-firing once. Their behaviour under the same test conditions as for other samples in this Part 6 experiment, is shown in Figure 22 for the dry condition. Although both samples suffered breakdown at 400V dc, the insulation resistance up to that point remained above 2×10^{12} ohms.

Test sample A₂₉ was selected from among the eight test substrates that were subjected to a total of 3 re-firing operations, because its case history showed that all three short circuits on its array after processing had disappeared by the time it had been re-fired three times. The results for this sample are shown in Figure 23, which indicates that there is no significant degradation in performance, under dry or wet conditions, as far as insulation resistance is concerned. The value remained above 10^{13} ohms, and the dielectric strength was greater than 500V dc for the sample.

Part 7.

The graph shown in Figure 24 indicates that the unit-area capacitance for System 'A' is $1.9 \text{ pF}\cdot\text{mm}^{-2}$ compared with $1.6 \text{ pF}\cdot\text{mm}^{-2}$ for System 'B'. Since the print thickness has a mean value of 46 microns for the dielectric, this would mean that for System 'A' the dielectric constant has a mean value of 10, and for System 'B' a mean value of 8, both measured at 1MHz and 22°C.

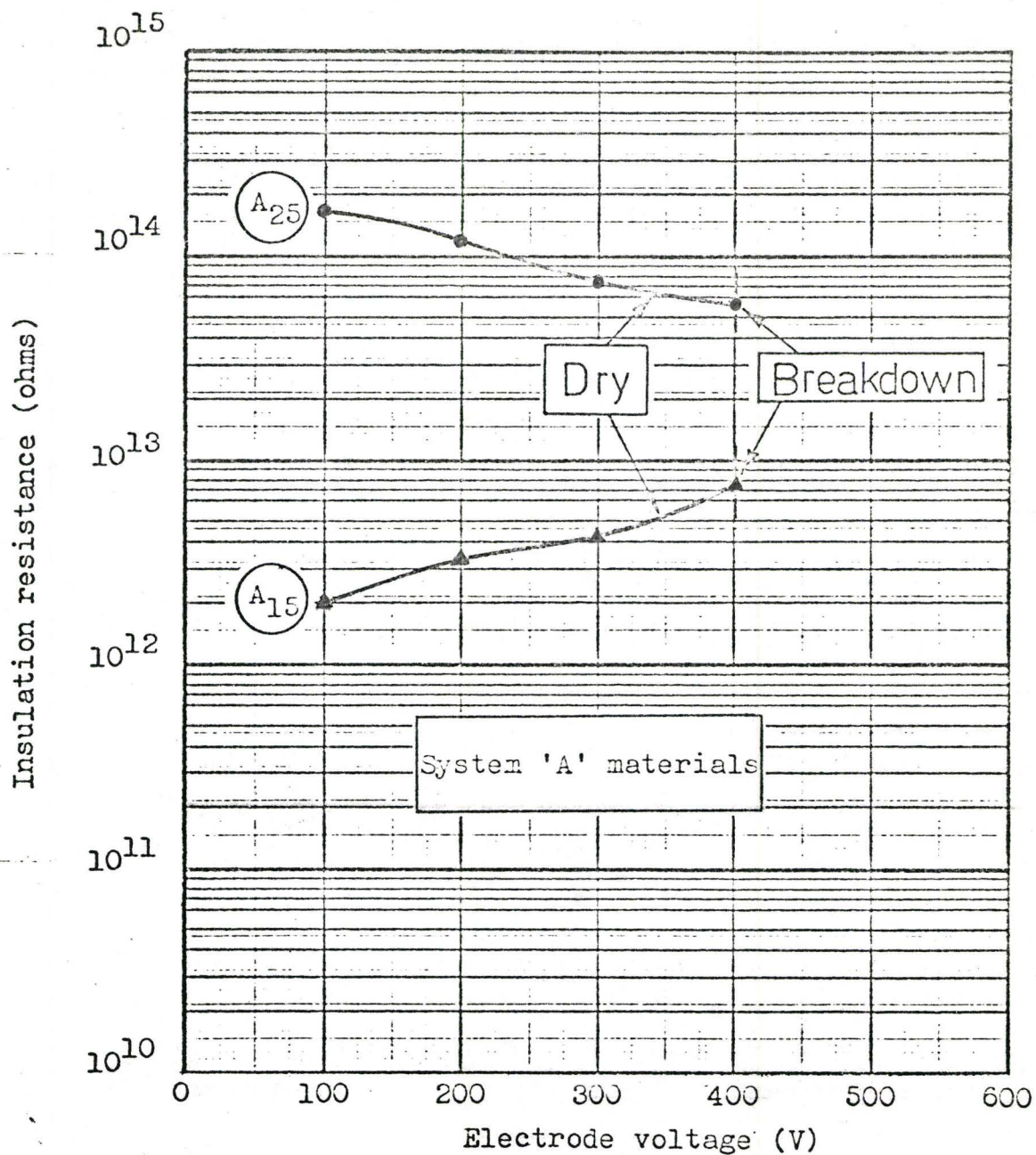


Figure 22. Effects of re-firing once on samples which had previously a short-circuit.

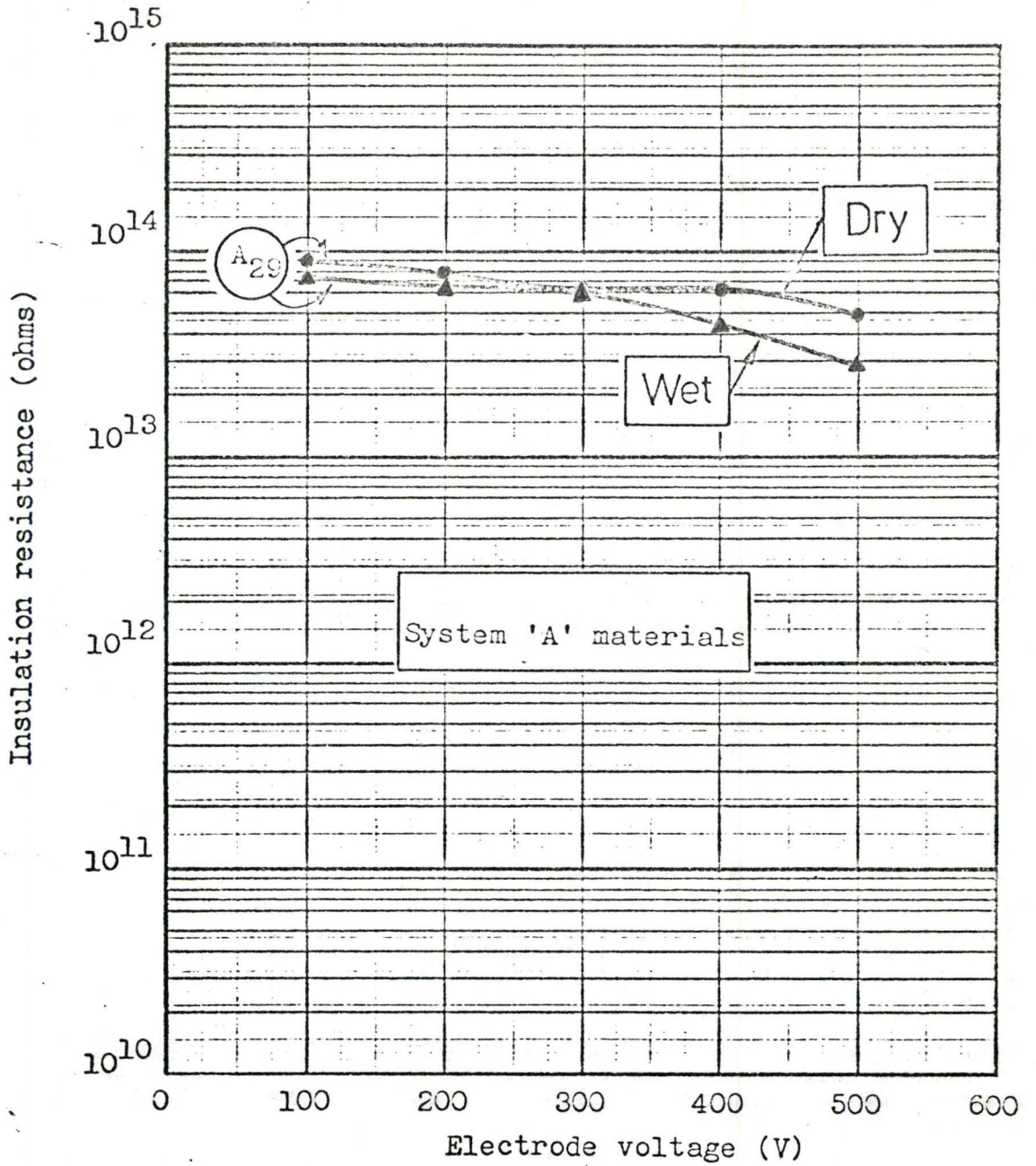


Figure 23. Effect of re-firing three times on insulation resistance.

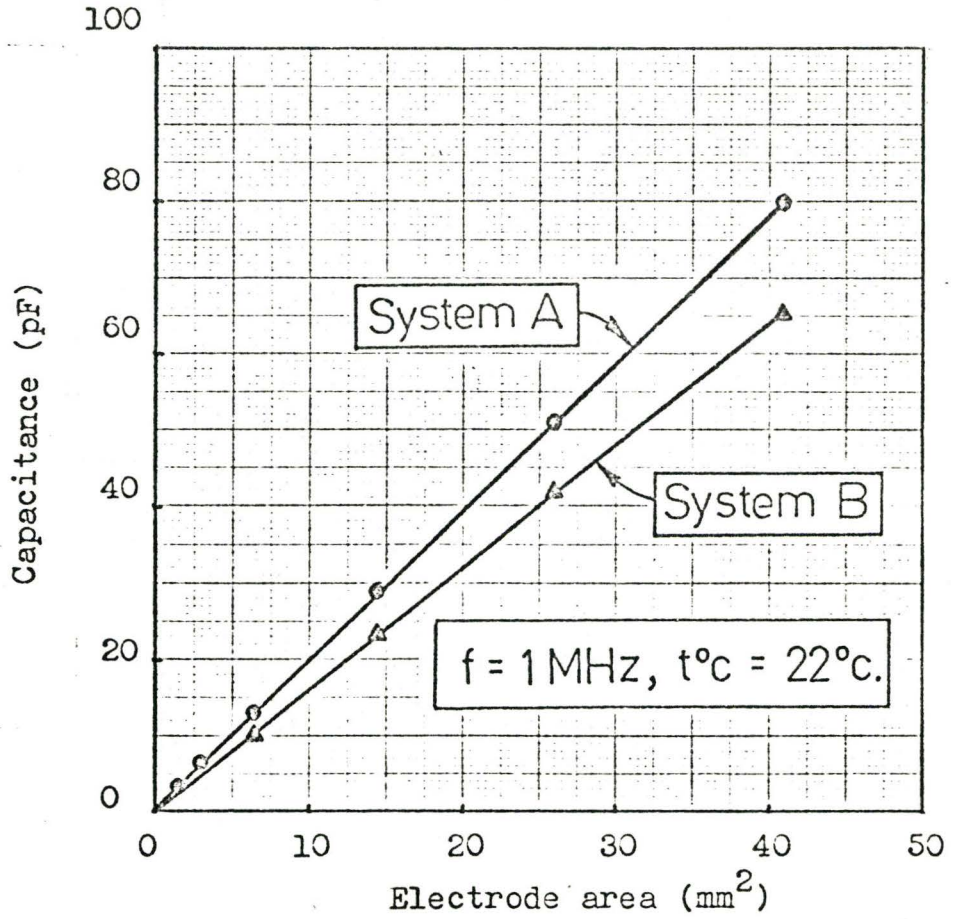


Figure 24. Unit-area capacitance for System 'A' and System 'B'.

The choice of processing option did not have a significant effect upon the values obtained for the capacitance of larger crossovers (pads K through N) and capacitors (pads A through J) of known geometry.

Part 8.

The drift in value of capacitance as a result of normal aging over a period of three months at ambient temperature (22°C), was determined for the large crossovers and capacitors referred to above. The results are plotted in Figure 25, and indicate that the drift is approximately +1.5% measured at 1MHz, for a typical test substrate.

Part 9.

The effect of re-firing once on the capacitance values obtained after processing appears to be an increase of between 2 and $3\frac{1}{2}\%$ measured at 1MHz and 22°C . The results are shown on the graph of Figure 26, for a typical test substrate.

Part 10.

The way in which the dielectric constant varied as a function of frequency for both systems was compared in the graph of Figure 27. For both systems, the dielectric constant varies insignificantly over almost three decades of frequency, with the value for System 'A' remaining approximately 20% higher throughout than System 'B'.

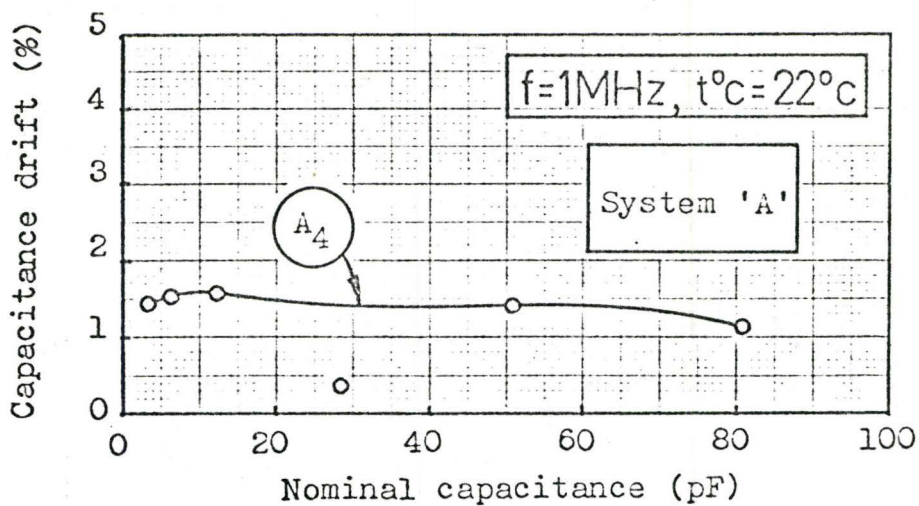


Figure 25. Aging effects over a period of three months.

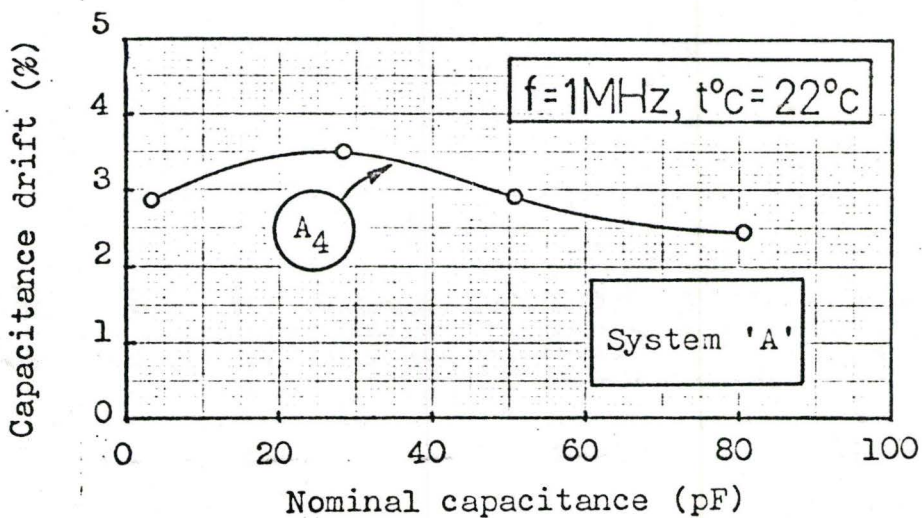


Figure 26. Effect of re-firing once on nominal capacitance values.

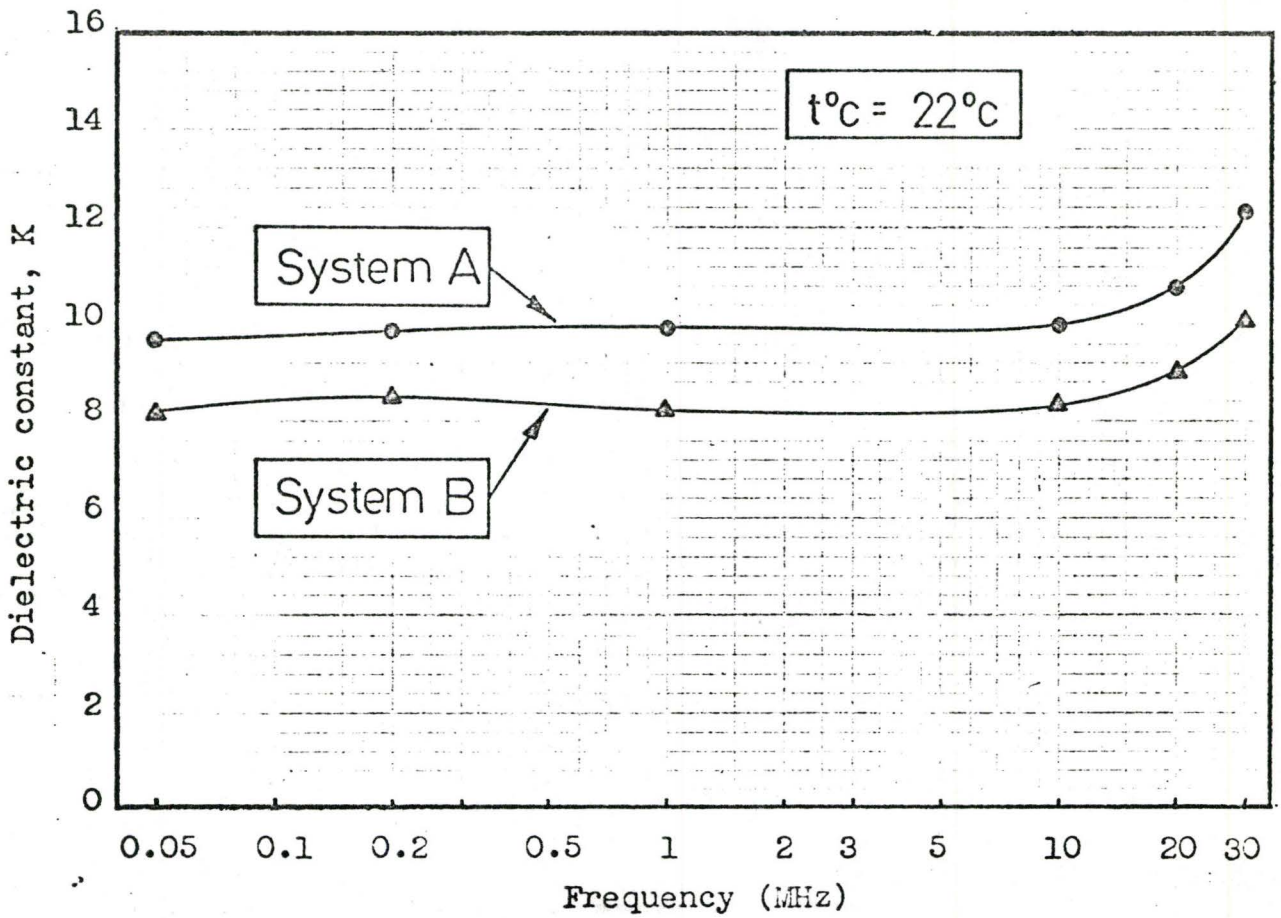


Figure 27. Variation of dielectric constant with frequency.

Part 11.

Results for the measurement of dissipation factor did not appear to be significantly affected by the processing option chosen, but did vary according to the size of pad chosen for measurement as illustrated in Figure 28. The plotted points have a measurement error of $\pm 10\%$, so there is some room for speculation regarding the true shape of the graphs, particularly for System 'B', since the higher loss component prevents more accurate determination of the null point in Q-meter measurements.

However, it seems clear that the dissipation factor is lowest in the region around 1MHz for System 'A', and becomes substantially higher at both lower and higher frequencies for both systems. Typical values of $\tan \delta$ for System 'A' at 1MHz are 0.1% and for System 'B', approximately 1%.

The dashed line in Figure 28 represents the loss curve that would be expected from the model of Figure 4, with values of $C_x = 80\text{pF}$, $R_s = 0.24\text{ ohms}$ and $R_p = 10\text{M}\Omega$, appropriate for pad E, System 'A'. Curve-fitting was not used for System 'B' in view of the inaccuracy of the results in this particular case. However, the general shape of the curves lends some support for the validity of the model.

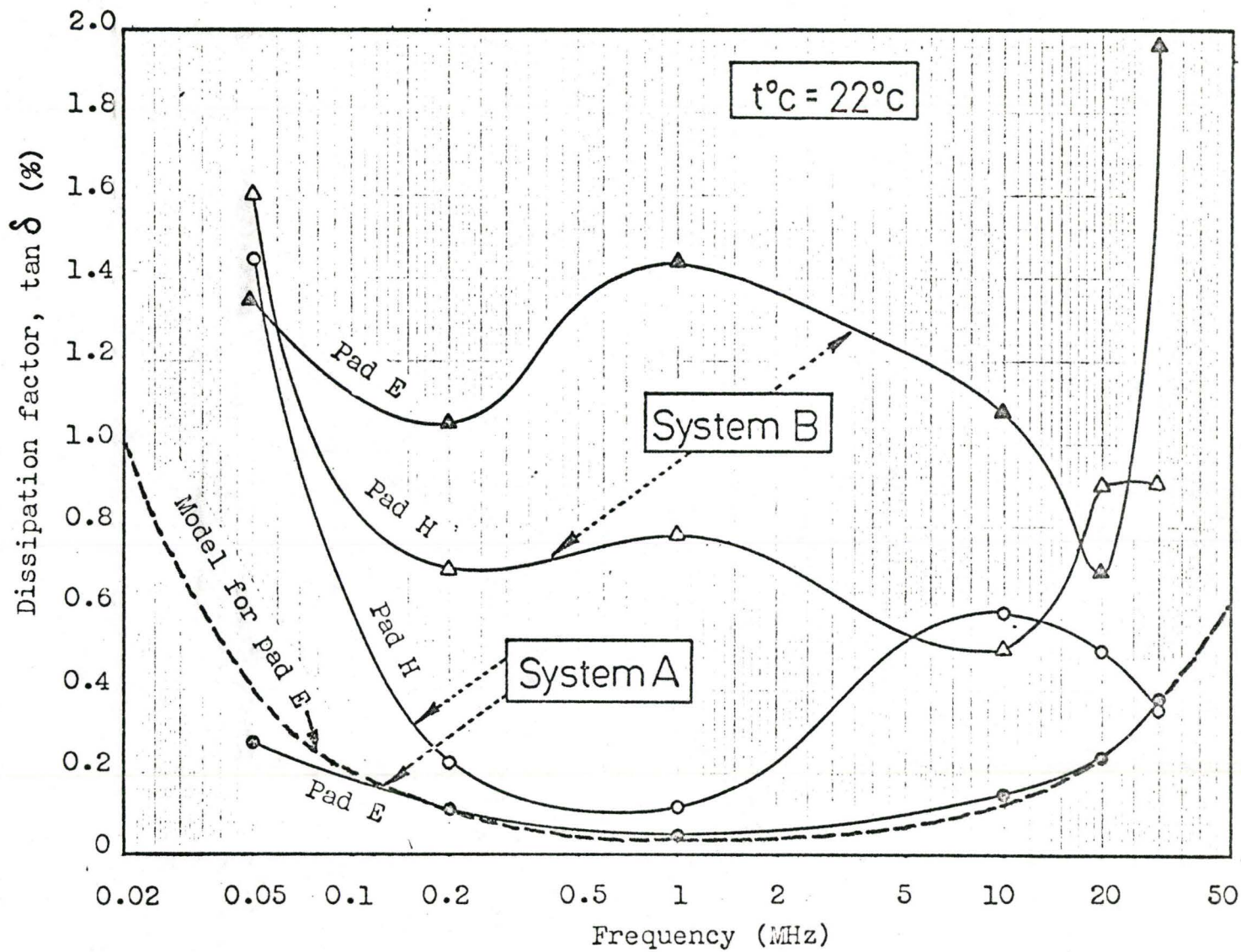


Figure 28. Variation in ac loss with frequency.

CONCLUSIONS

A study of Part 1 results leaves little doubt that the method of manufacture strongly influences the circuit yield and that there is a best choice of processing option for each system. In this case, it would be Option 2(a) for System 'A' and Option 1(b) for System 'B'. Care must be taken to ensure a realistic interpretation of the yield figures given here because, in the case of a production circuit, (as opposed to an array of very closely spaced crossovers to test the practical limitations of the process) actual yield depends on processing care and circuit complexity. The probability of obtaining 100% yield decreases exponentially with the product of defect density and active circuit area. If circuit yield is to be the prime consideration, then circuit designs must exploit this situation where possible.

There is a strong indication from the results that the effect of re-firing has a tendency to change the location of short-circuits that may appear immediately after processing. Some seem to be eliminated altogether, and others formed elsewhere on the arrays of various test substrates. Of the 22 test substrates, 10 showed an increase in the number of short-circuits per array while 10 showed a decrease, and 2 had no change. After being re-fired a total of three times,

there was an overall increase in yield. This may have been due to there being sufficient thermal energy available to cause a break in some, or indeed all, of the tenuous conducting paths resulting from diffusion of conducting ions into the dielectric from the crossover electrodes. Some support for this proposal might be found in the case history of sample A₂₉, which had three short-circuits on its array after processing, one after being re-fired once, and none at all after being re-fired three times. Figure 23 indicates that the effect of re-firing does not degrade its performance relative to the other test substrates with no such case history.

On an overall basis, the effect of re-firing on either System 'A' or System 'B' materials is unlikely to affect the yield, insulation resistance, dielectric strength or dielectric constant values to any significant degree.

There is no question about the superiority of System 'A' materials over System 'B' as far as dielectric strength is concerned, and leads to the rejection of the latter on the basis of it not being impervious to moisture. It would require the use of a protective overglaze if high humidity conditions were to be encountered. Furthermore, breakdown voltages of the order of 150V dc, and insulation resistance values falling to a few megohms would be quite unsatisfactory for good crossovers. By contrast, System 'A' materials are quite capable of sustaining electrode voltages in excess of 200V dc, and in fact, 70% of the samples could sustain 500V dc. Since

the insulation resistance remained above 10^{12} ohms under both dry and wet conditions, it appears to be practically impervious to water and would not require overglazing. It is to be recommended as a most suitable dielectric for crossover applications.

It should be made clear that insulation resistance tests could only be conducted on samples that had no short-circuits on their arrays (so that 100 crossovers could be used in parallel), or those samples having so few short-circuits that a sample could be prepared avoiding the rows and columns affected. In the latter case, at least 80 crossovers were paralleled for a usable sample. The validity of the results is based on the premise that each crossover behaves similarly, the total leakage current being equally divided among them. From an analysis of the failures after insulation resistance tests, it appeared unlikely that breakdown had occurred simultaneously in a given sample of crossovers; most probably the weakest crossover initiated the breakdown. For this reason, the dielectric strength measurements were conducted on single crossovers selected at, or near, the centre of the array of crossovers.

During the course of the experiments on dielectric strength, an interesting effect occurred. When an existing short-circuit was exposed to a very high electric field, for example, 600V dc across 46 microns of dielectric, it could be made to go open circuit in some cases. It often

occured for electrode voltages of the order of 100V dc, and subsequent measurement of the insulation resistance yielded values in excess of 10^7 ohms.

Although the behaviour was unsystematic, this effect should be investigated with a much larger sample set, because a voltage 'burn-in' period for crossovers might conceivably be used to improve the yield situation. This effect was discussed under the heading DC Effects, in the DISCUSSION section of the report.

It was evident from the results obtained, that the dielectric constant of both systems was sufficiently low (i.e. <10), and relatively independent of frequency, that the coupling capacitance of normal sized crossovers ($<1\text{mm}^2$) would be under 0.5pF. Furthermore, the option chosen for processing did not appear to have any significant effect on the value obtained for dielectric constant, and the drift to be expected as a result of normal aging and/or re-firing several times, is likely to be no more than 3%.

The dissipation factor was substantially less for System 'A' than for System 'B', 0.1% as opposed to 1% at 1MHz, which indicates the superiority of System 'A' when used to process low value (i.e. $\approx 100\text{pF}$), low-loss capacitors. Again, the values obtained for $\tan \delta$ did not appear to be affected significantly by the processing option chosen.

RECOMMENDATIONS

1. Adoption of System 'A' materials for further experimentation on larger samples of test substrates in the area of reliability, using specific production circuits of known multilayer geometry.
2. To ensure as high a yield as possible, extreme cleanliness is essential in all stages of processing dielectrics. Inspect all substrates after each printing stage, and again after each firing process, to detect any foreign matter which might become embedded in the dielectric layer. If possible, one printer should be assigned only for the production of dielectric prints to avoid the possibility of carry-over of conductive and/or resistive material on the squeegees. Dust covers should be used over fresh prints if there is likely to be delays before firing.
3. There is some evidence to suggest that re-firing several times might be used deliberately to improve the yield. The integrity of the dielectric need be checked only at the end of the complete firing sequence, as earlier checks are very likely to be inconclusive. If existing

short-circuits are found to disappear at some later stage of firing, and remain open circuit until completion of the processing sequence, there seems to be no reason why that circuit should not function as well as those with no past history of faults at any stage.

4. Instrumentation capable of directly indicating nano-ampere leakage currents should be obtained if the relative merits of other paste systems are to be evaluated in the future. A direct-reading capacitance meter should be available in the laboratory facility.

A well-regulated high-voltage dc supply should be obtained for making measurements on insulation resistance, as poor regulation gives rise to a current component indistinguishable from leakage and absorption currents; the voltage must be monitored directly.

APPENDIX

Q-meter measurement of Capacitance and AC loss in terms of an equivalent parallel R-C circuit

1. The Q-meter circuit is illustrated in Figure 29. The output level of the oscillator is adjusted to a suitable reference level at the chosen test frequency, ω .
2. A suitable inductor is chosen that resonates at the chosen test frequency with the calibrated standard tuning capacitor at about mid-range (C_1), and the circuit 'Q' is indicated directly on the EVM. (Q_1)
3. The component whose impedance is expected to be primarily due to capacitive reactance, is connected across the test terminals of the meter. The tuning capacitor is adjusted for resonance again, (C_2), and there is a decrease, ΔQ , in the value of circuit 'Q'. (Q_2)
4. Let R and C represent the equivalent parallel elements of the unknown component. The following expressions are easily obtained:

$$C = C_1 - C_2 ; \quad R = \frac{Q_1 Q_2}{\Delta Q \cdot \omega C_1} ; \quad \tan \delta = \frac{C_1}{C_1 - C_2} \cdot \frac{\Delta Q}{Q_1 Q_2} ;$$

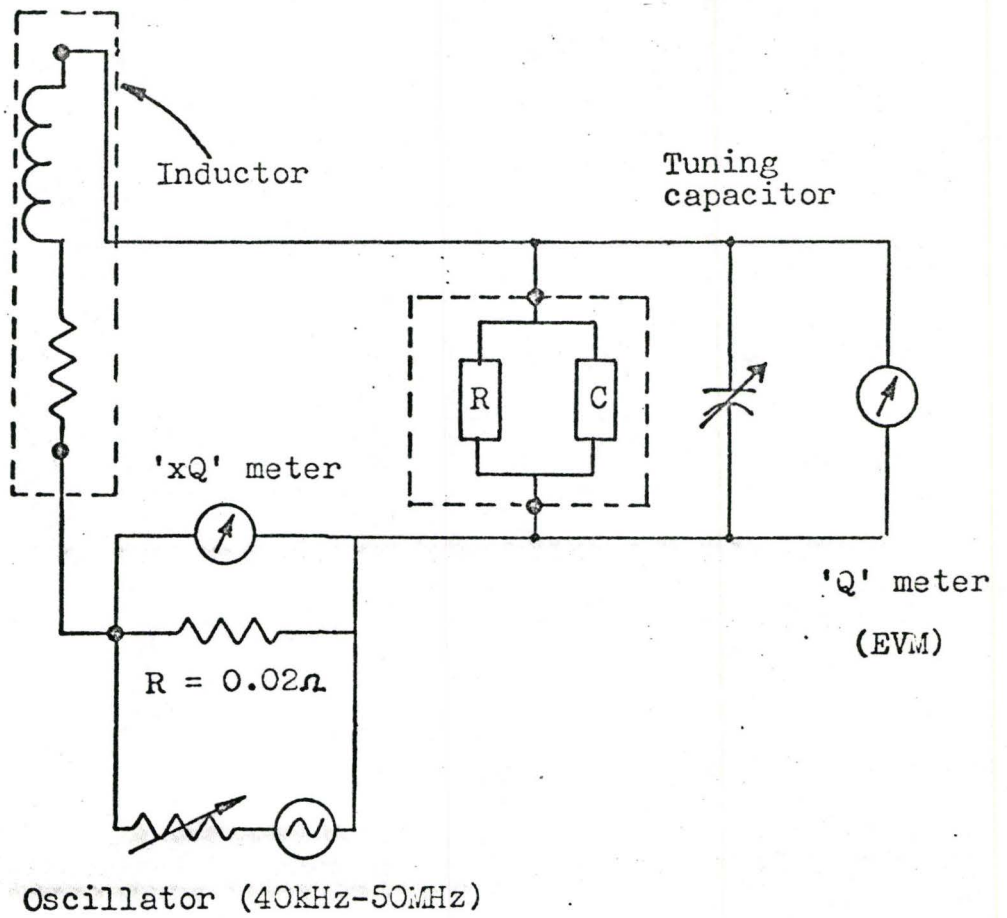


Figure 29. The Q-meter circuit.

REFERENCES

1. L.C. Hoffman, "Crystallizable Dielectrics," Hybrid Microelectronics Symposium, Oct. 1968, pp. 111-118.
2. J.P. Holden, "The Development of Glaze Capacitors for Thick Film Circuits," I.E.R.E. Conference Proceedings #11, April 1968, pp. 61-72.
3. T. Nakayama and L.C. Hoffman, "Performance Data on Thick-Film Crossovers," I.E.R.E. Conference Proceedings #11, April 1968, pp. 133-142.
4. S.J. Stein, C. Huang, L. Cang, and G. Schultz, "Recent Advances in Platinum-Silver Thick Film Conductors," Electro-Science Laboratories, Inc. Pennsauken, N.J.
5. N.P. Bogoroditskii and V.V. Pasyukov, "Radio and Electronic Materials," Iliffe Books Ltd, Translation: Scripta Technica Ltd, G.B., 1967.
6. W.D. Cooper, "Instrumentation and Measurement Techniques," Prentice-Hall Inc., 1970.
7. Bell Telephone Labs. Inc., "Physical Design of Electronic Systems," vol. II, Prentice-Hall Inc., 1970.
8. C.A. Harper (Editor), "Handbook of Thick-Film Hybrid Microelectronics," McGraw-Hill Inc., 1974.